Electronic Supplementary Material (ESI) for RSC Advances.

Supporting Information

Aryl Sulfonate Anion Stabilized Aromatic Triangular Cation $[Pd_3]^+$: Syntheses, Structures and Properties

Miaomiao Wang, Zhixin He, Meng Chen, Yanlan Wang*

1. General remarks

All reagents used as starting materials in the syntheses were purchased from commercial sources. Chloroform was dewatered using a dewatering system, but it did not need to be treated with bases. Reactions and filtrations were carried out under N_2 using standard Schlenk technique. ^{1}H NMR spectra and ^{13}C NMR spectra were recorded at 300K on a Varian spectrometer (500M) using TMS as internal standard (0.00 ppm for ^{1}H NMR and 77.00 ppm for ^{13}C NMR for $CDCl_3$). ^{13}C NMR spectra were recorded at 125 MHz. For ^{31}P NMR, H_3PO_4 was used as external standards (0.00 ppm). ^{19}F NMR spectra were recorded at 471 MHz. Exact masses were recorded on a high resolution tandem time LC/MS instrument (G2-XSQTOF Mass Spectrometry). X-ray photoelectron microscopy (XPS) spectra were conducted on a Thermo Escalab Xi using a monochromate Al X-ray resource at 1486.6 eV with a C1s 284.0 eV reference. Fourier Transform Infrared Spectrometer (FTIR) of these complexes was recorded on a IRTracer-100 Fourier Transform. Absorbance spectra measurements were performed on a T9CS UV–vis spectrophotometer (Persee Instrument Co., Ltd. Beijing, China). The fluorescence spectra in solutions were measured on F-7100 spectrofluorimeter (Hitachi, Japan) luminescence spectrophotometer at room temperature under the following conditions: excitation wavelength = 250 nm, excitation and emission slit width of 5 nm. The absolute fluorescence quantum yields (PLQY) were determined with a FLS1000 steady-state transient fluorescence spectrometer in CH_3OH, CH_3CN, CH_3COCH_3, $CHCl_3$ and THF under an air atmosphere at room temperature (1×10^{-4} M, λ_{ex} = 250 nm). The PLQY were determined by using calibrated integrated sphere Quanta-φ (FLS1000) in solvents.

2. Experimental procedures

Synthesis of substituted aromatic silver sulfonates

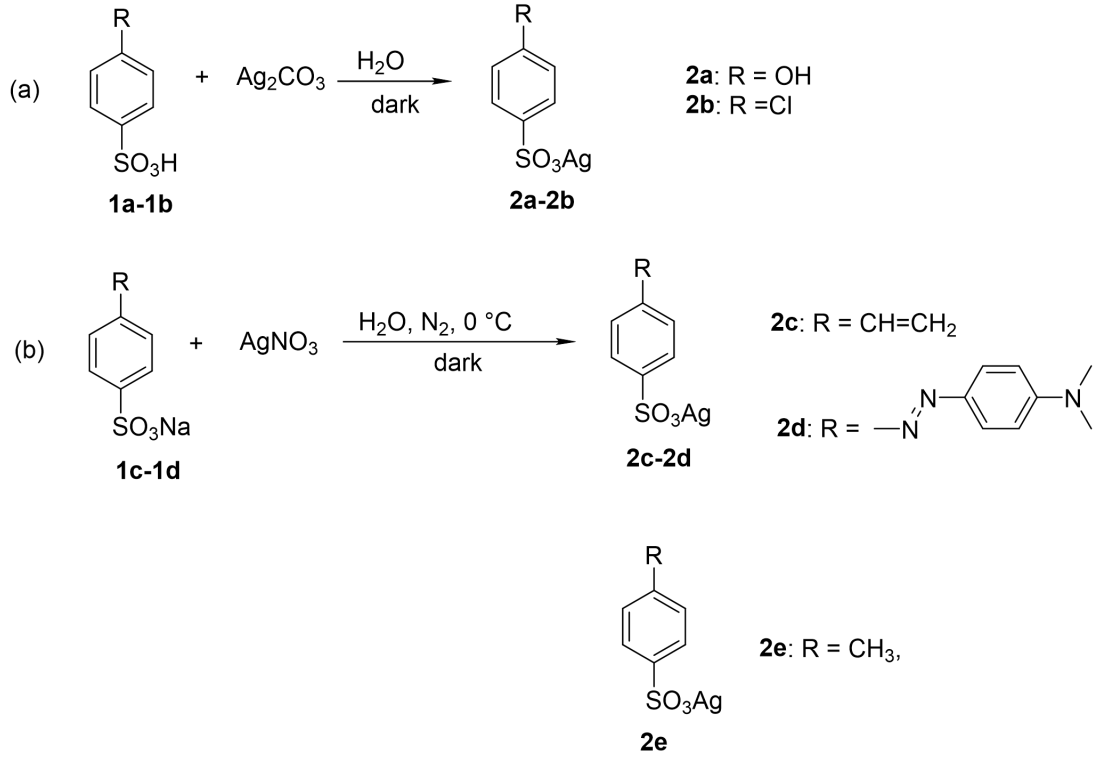

Scheme S1. Two methods for the synthesis of substituted aromatic silver sulfonates.

We synthesized substituted silver aromatic sulfonates using the following two methods in Scheme S1(**a** and **b**).

Method a: For example, 4-hydroxybenzenesulfonic acid (1.145 mmol, 200 mg, 1 equiv.) was dissolved in 3 mL deionized water, then Ag_2CO_3 (0.687 mmol, 189.4 mg, 1.2 equiv.) was added and the mixture was stirred for 2 h in the dark. After filtration, the deionized water was removed by a rotary evaporator, and the obtained pale violet solid **2a** was dried in a vacuum oven overnight (Yield = 99％). White solid **2b** was also prepared using the same method (Yield = 84％).

Method b: For example, sodium 4-vinylbenzenesulfonate (0.97 mmol, 200 mg, 1 equiv.) was dissolved in 3 mL deionized water, 0.5 mL $AgNO_3$ (0.97 mmol, 164.8 mg, 1 equiv.) was added dropwise at 0 ℃, and the reaction mixture was stirred in the dark for 2 h. After filtration, the grey purple solid **2c** was dried in a vacuum oven overnight (Yield = 76％). The deep red solid **2d** was also prepared using similar method (Yield = 74％).

Synthesis of complexes 3-7

The syntheses of complexes **3-7** has been carried out according to the following procedure. $Pd(dba)_2$ (0.2 mmol, 115 mg, 1 equiv.) was added to a 50 mL Schlenk. The vessel underwent at least three vacuum/N_2 cycles. 20 mL of freshly degassed $CHCl_3$ were then syringed under N_2. The phosphine (0.2 mmol, 1 equiv.) and the bis(4-chlorophenyl) disulfide (0.1 mmol, 0.5 equiv.) were immediately added to the mixture under N_2. The resulting solution was kept under stirring at r.t. for 2 hours, the aryl silver sulfonates (0.067 mmol, 0.33 equiv.) was then added under N_2 and the solution was maintained stirring for 1 hour in the dark. Then, the mixture was filtered through a short pad of celite under N_2 to remove trace of black precipitations. The solvent was removed under vacuum to leave a deep red solid that was further purified by $CHCl_3$/hexane precipitations for three times (each time, 1/30 v/v, 3×30 mL). After evaporation of solvents under vacuum afforded products as orange/red solids. These products were further purified by recrystallization by vapor diffusion method using $CHCl_3$/hexane. Through this method, crystals of complex **7** suitable for X-Ray diffractions were obtained. Complexes **3-7** were fully characterized by ^{1}H, ^{13}C, ^{31}P and ^{19}F NMR, UV-vis., XPS, and HRMS.

X-ray crystallography

Single crystal X-ray diffraction data of complex **7** (CCDC: 2270588) was collected with an Agilent Xcalibur CCD diffractometer (Gemini E/Eos) at 293(2) K with Cu Kα radiation (λ = 1.54184 Å). The data were integrated and corrected for Lorentz and polarization effects using SAINT.[1] The absorption corrections were applied with SADABS.[2] The structures was solved by direct method through SHELXS-2014[3] and refined by full-matrix least-squares method on F^2 using the SHELXTL crystallographic software package.[4] Non-hydrogen atoms are refined by anisotropic temperature parameters. The hydrogen atoms were placed in the calculated positions using isotropic thermal displacement parameters. Details of crystal data are listed in Table S1, and selected bond lengths and bond angles are provided in Table S2.

3. Spectroscopic data

3.1 Spectroscopic data for substituted aromatic silver sulfonates (2a-2d)

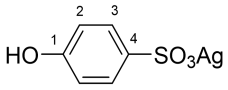

Silver 4-hydroxybenzenesulfonate. (2a) Yield = 99%, pale violet solid, HRMS calculated for $C_6H_5O_4S^-$ 173.0014, found 173.0012. ^{1}H NMR (500 MHz, DMSO-d_6) δ 9.56 (s, 1H), 7.43 (d, *J* = 8.5 Hz, 2H), 6.68 (d, *J* = 8.5 Hz, 2H). ^{13}C NMR (125 MHz, DMSO-d_6) δ 158.08(C1), 139.41(C4), 127.61(C2), 114.54(C3).

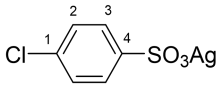

Silver 4-chlorobenzenesulfonate. (2b) Yield = 84%, white solid, HRMS calculated for $C_6H_4ClO_3S^-$ 190.9691, found 190.9695. ^{1}H NMR (500 MHz, DMSO-d_6) δ 7.62 (d, *J* = 8.5 Hz, 2H), 7.40 (d, *J* = 8.4 Hz, 2H). ^{13}C NMR (125 MHz, DMSO-d_6) δ 147.47(C4), 133.54(C1), 128.21(C2), 127.96(C3).

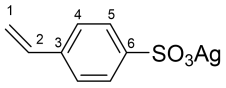

Silver 4-Vinylbenzenesulfonate. (2c) Yield = 76%, grey purple solid, HRMS calculated for $C_8H_7O_3S^-$ 183.0221. found 183.0226. ^{1}H NMR (500 MHz, DMSO-d_6) δ 7.57 (d, J = 8.1 Hz, 2H), 7.43 (d, J = 8.0 Hz, 2H), 6.73 (dd, J = 17.7, 10.9 Hz, 1H), 5.85 (d, J = 17.6 Hz, 1H), 5.28 (d, J = 10.9 Hz, 1H). ^{13}C NMR (125 MHz, DMSO-d6) δ 147.86(C6), 137.75(C3), 136.58(C2), 126.33(C5), 126.00(C4), 115.25(C1).

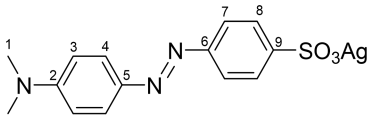

(E)-**(((4-((4-(dimethylamino)phenyl)diazenyl)phenyl)sulfonyl)oxy)silver. (2d)** Yield = 74%, deep red solid, HRMS calculated for $C_{14}H_{14}N_3O_3S^-$ 304.0908, found 304.0901. ^{1}H NMR (500 MHz, DMSO-d_6) δ 7.72-7.80 (m, 6H), 6.82 (d, *J* = 8.7 Hz, 2H), 3.04 (s, 6H). ^{13}C NMR (125 MHz, DMSO-d_6) δ 153.12(C6), 152.82(C2), 148.66(C9), 142.98(C5), 127.05(C8), 125.37(C4), 121.73(C7), 112.01(C3), 40.27(C1).

3.2 Spectroscopic data for complexes 3-7

Complex 3

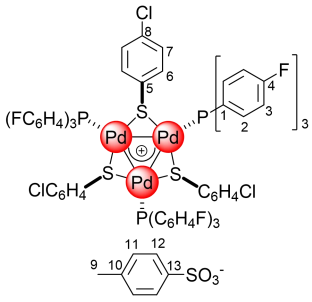

Yield = 92%, orange solid, HRMS calculated for $C_{72}H_{48}P_3Pd_3S_3Cl_3F_9^+$ 1698.7048, found 1698.7056. HRMS calculated for $C_7H_7O_3S^-$ 171.0161, found 171.0169. ^{1}H NMR (500 MHz, $CDCl_3$) δ 7.88 (d, J = 7.7 Hz, 2H), 7.21-7.07 (m, 20H), 6.86 (t, J = 8.4 Hz, 18H), 6.76 (d, J = 8.0 Hz, 6H), 6.47 (s, 6H), 2.36 (s, 3H). ^{31}P NMR (202 MHz, $CDCl_3$) δ 13.41. ^{13}C NMR (125 MHz, $CDCl_3$) δ 164.14 (d, J = 254.0 Hz, C4), 145.41 (C13), 138.34 (C10), 136.04 (C6), 135.77 (d, J = 9.7, 4.7 Hz, C2), 134.23 (C8), 134.10 (C5), 128.77 (C7), 128.38 (C11), 127.08-126.54 (m, C1), 126.34 (C12), 115.93 (d, J = 21.5, 3.9 Hz, C3), 21.25 (C9). ^{19}F NMR (471 MHz, $CDCl_3$) δ -107.77.

Complex 4

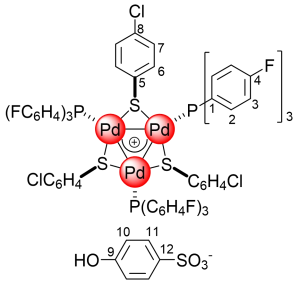

Yield = 92%, orange solid, HRMS calculated for $C_{72}H_{48}P_3Pd_3S_3Cl_3F_9^+$ 1698.7048, found 1698.7072. HRMS calculated for $C_6H_5O_4S^-$ 172.9957, found 172.9959. ^{1}H NMR (500 MHz, $CDCl_3$) δ 7.68 (d, J = 8.2 Hz, 2H), 7.14 (s, 18H), 6.88 (t, J = 8.4 Hz, 18H), 6.74 (d, J = 8.0 Hz, 6H), 6.62 (d, J = 8.3 Hz, 2H), 6.39 (d, J = 8.0 Hz, 6H). ^{31}P NMR (202 MHz, $CDCl_3$) δ 13.36. ^{13}C NMR (125 MHz, $CDCl_3$) δ 164.13 (d, J = 254.0 Hz, C4), 157.31 (C9), 139.30 (C12), 135.96 (C6), 135.74 (d, J = 9.5, 5.0 Hz, C2), 134.34 (C8), 134.19 (C5), 128.67 (C7), 127.75 (C10), 127.09-126.57 (m, C1), 115.93 (d, J = 21.4, 3.9 Hz, C3), 115.16(C11). ^{19}F NMR (471 MHz, $CDCl_3$) δ -107.64.

Complex 5

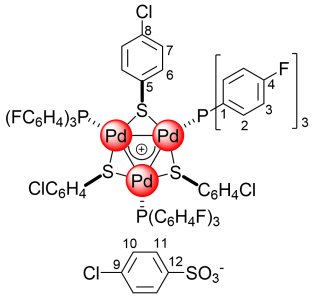

Yield = 92%, orange solid; HRMS calculated for $C_{72}H_{48}P_3Pd_3S_3Cl_3F_9^+$ 1698.8362, found 1698.8303. HRMS calculated for $C_6H_4ClO_3S^-$ 190.9625, found 190.9623. ^{1}H NMR (500 MHz, $CDCl_3$) δ 7.90 (d, *J* = 8.2 Hz, 2H), 7.28 (s, 2H), 7.13 (s, 18H), 6.88 (t, *J* = 8.4 Hz, 18H), 6.77 (d, *J* = 8.0 Hz, 6H), 6.41 (d, *J* = 8.0 Hz, 6H). ^{31}P NMR (202 MHz, CDCl3) δ 13.42. ^{13}C NMR (125 MHz, $CDCl_3$) δ 163.17 (d, *J* = 254.3 Hz, C4), 145.72 (C12), 134.94 (C6), 134.69 (d, *J* = 9.4, 4.7 Hz, C2), 133.32 (C8), 133.29 (C5), 133.12 (C9), 127.76 (C7), 126.97 (C10), 126.81 (C11), 125.76 (dr, *J* = 34.5, 12.9 Hz, C1), 114.98 (d, *J* = 21.8, 4.1 Hz, C3). ^{19}F NMR (471 MHz, $CDCl_3$) δ -107.50.

Complex 6

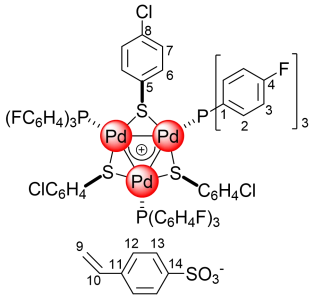

Yield = 92%, orange solid, HRMS calculated for $C_{72}H_{48}P_3Pd_3S_3Cl_3F_9^+$ 1698.7048, found 1698.7067. HRMS calculated for $C_8H_7O_3S^-$ 183.0161, found 183.0165. ^{1}H NMR (500 MHz, $CDCl_3$) δ 7.94 (d, *J* = 8.2 Hz, 2H), 7.37 (d, *J* = 8.2 Hz, 2H), 7.14 (s, 18H), 6.87 (t, *J* = 8.6 Hz, 18H), 6.79–6.70 (m, 7H), 6.45 (d, *J* = 8.0 Hz, 6H), 5.75 (dd, *J* = 17.5, 1.0 Hz, 1H), 5.25 (dd, *J* = 11.0, 1.0 Hz, 1H). ^{31}P NMR (202 MHz, $CDCl_3$) δ 13.45. ^{13}C NMR (125 MHz, $CDCl_3$) δ 164.15 (d, *J*=254.2 Hz, C4), 147.58 (C14), 137.83(C11), 136.73 (C10), 136.01 (C6), 135.92-135.60 (m, C2), 134.28 (C8), 134.12 (C5), 128.78 (C7), 126.97 (C1), 126.64 (C13), 125.72 (C12), 116.13-115.77 (m, C3), 113.96(C9). ^{19}F NMR (471 MHz, $CDCl_3$) δ -107.66.

Complex 7

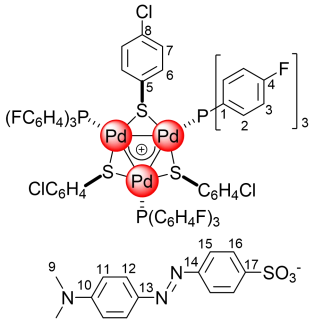

Yield = 92%, red solid, HRMS calculated for $C_{72}H_{48}P_3Pd_3S_3Cl_3F_9^+$ 1698.7048, found 1698.7059. HRMS calculated for $C_{14}H_{14}N_3O_3S^-$ 304.0801, found 304.0802. ^{1}H NMR (500 MHz, $CDCl_3$) δ 8.08 (d, *J* = 8.3 Hz, 2H), 7.89 (d, *J* = 8.8 Hz, 2H), 7.80 (d, *J* = 8.2 Hz, 2H), 7.14 (s, 18H), 6.87 (t, *J* = 8.4 Hz, 18H), 6.77 (b, 8H), 6.44 (d, *J* = 8.0 Hz, 6H), 3.09 (s, 6H). ^{31}P NMR (202 MHz, $CDCl_3$) δ 13.20. ^{13}C NMR (125 MHz, $CDCl_3$) δ164.14 (d, *J* = 254.2 Hz, C4), 153.04 (C14), 152.38 (C10), 148.98 (C17), 143.83 (C13), 136.01 (C6), 135.76 (dt, *J* = 9.2, 4.8 Hz, C2), 134.26 (C5), 128.74 (C7), 127.17 (C16), 127.12-126.57 (m, C1), 124.95 (C12), 121.83 (C15), 115.94 (dq, *J* = 21.6, 4.1 Hz, C3), 111.52 (C11), 40.31 (C9). ^{19}F NMR (471 MHz, $CDCl_3$) δ -107.57.

4. XPS spectra for complexes 3-6

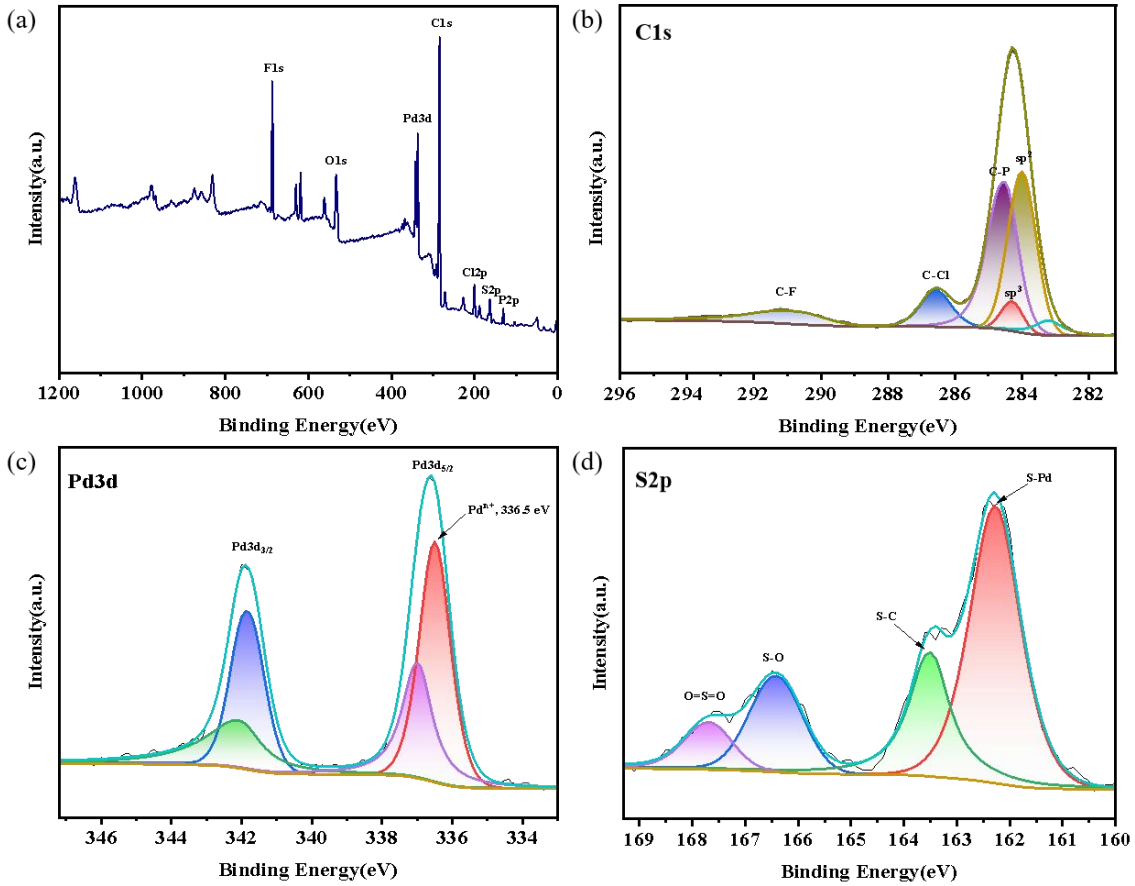

Fig. S1. (a) XPS survey spectrum of complex **3**, high-resolution (b) C 1s, (c) Pd 3d, (d) S 2p spectra of complex **3**.

For better understanding the bonding forms and valence states for complex **3**, we examined it by X-ray Photoelectron Spectroscopy (XPS). Firstly, the observed binding energies for their involved elements: Pd, C, O, S, Cl, P and F presented to be completely consistent with atoms in analogous structures and definitely manifested their existences (Fig. S1a). The high-resolution XPS spectrum for C1s in complex **3** presented five characteristic peaks at 284.00, 284.30, 284.50, 286.60, and 291.20 eV (Fig. S1b), which were ascribed to the sp^2 carbon, sp^3 carbon, C-P, C-Cl, and C-F, respectively. The XPS for Pd 3d in complex **3** showed two peaks at 336.50 and 341.90 eV , which were certainly assigned to Pd^{n+} $3d_{5/2}$ and Pd^{n+} $3d_{3/2}$, respectively (Fig. S1c). In addition, the high-resolution XPS spectrum for S2p presented four peaks at 162.30, 163.50, 166.40, and 167.70 eV, responding to the S-Pd, S-C, S-O, and O=S=O, respectively (Fig. S1d).

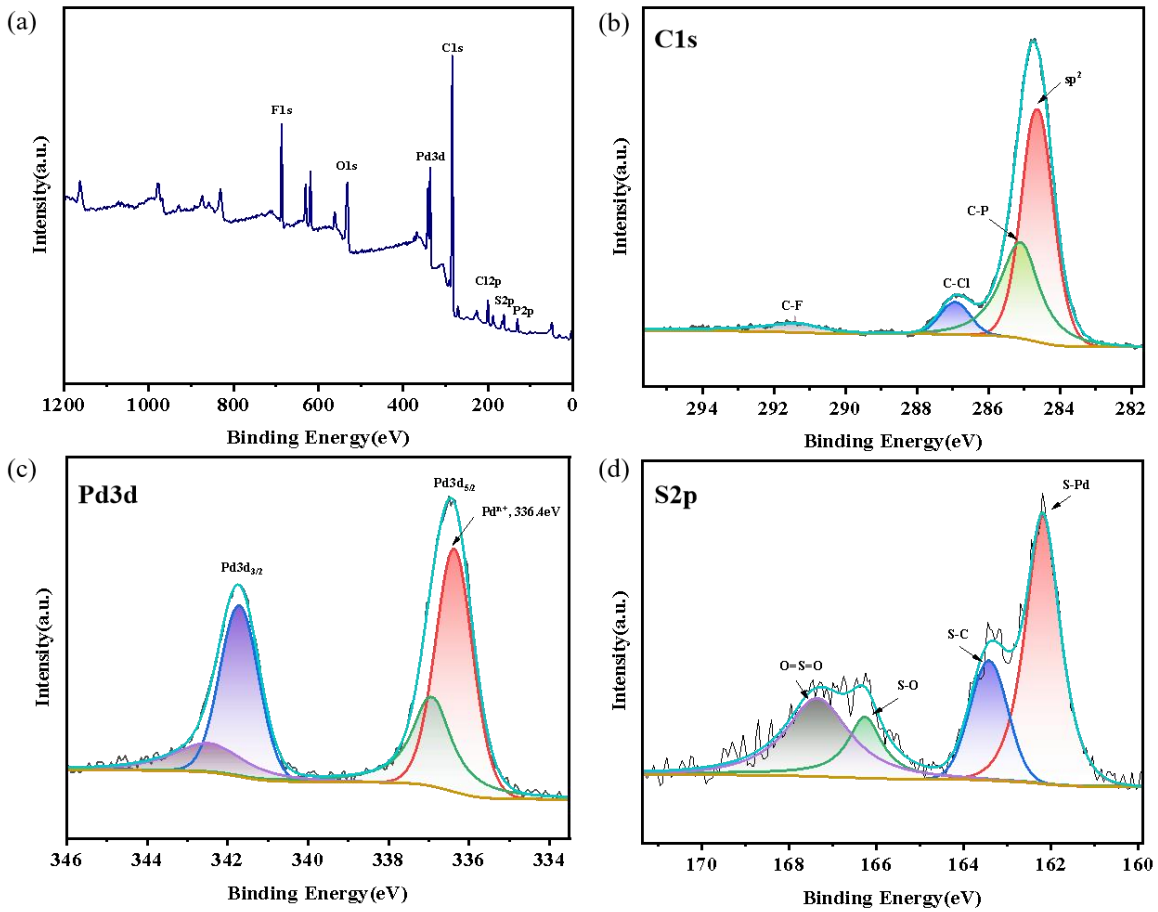

Fig. S2. (a) XPS survey spectrum of complex **4**, high-resolution (b) C 1s, (c) Pd 3d, (d) S 2p spectra of complex **4**.

For better understanding the bonding forms and valence states for complex **4**, we examined it by X-ray Photoelectron Spectroscopy (XPS). Firstly, the observed binding energies for their involved elements: Pd, C, O, S, Cl, P and F presented to be completely consistent with atoms in analogous structures and definitely manifested their existences (Fig. S2a). The high-resolution XPS spectrum for C1s in complex **4** presented four characteristic peaks at 284.65, 285.10, 286.95, and 291.40 eV (Fig. S2b), which were ascribed to the sp^2 carbon, C-P, C-Cl, and C-F, respectively. The XPS for Pd 3d in complex **4** showed two peaks at 336.40 and 341.70 eV , which were certainly assigned to Pd^{n+} $3d_{5/2}$ and Pd^{n+} $3d_{3/2}$, respectively (Fig. S2c). In addition, the high-resolution XPS spectrum for S2p presented four peaks at 162.20, 163.35, 166.25, and 167.35 eV, responding to the S-Pd, S-C, S-O, and O=S=O, respectively (Fig. S2d).

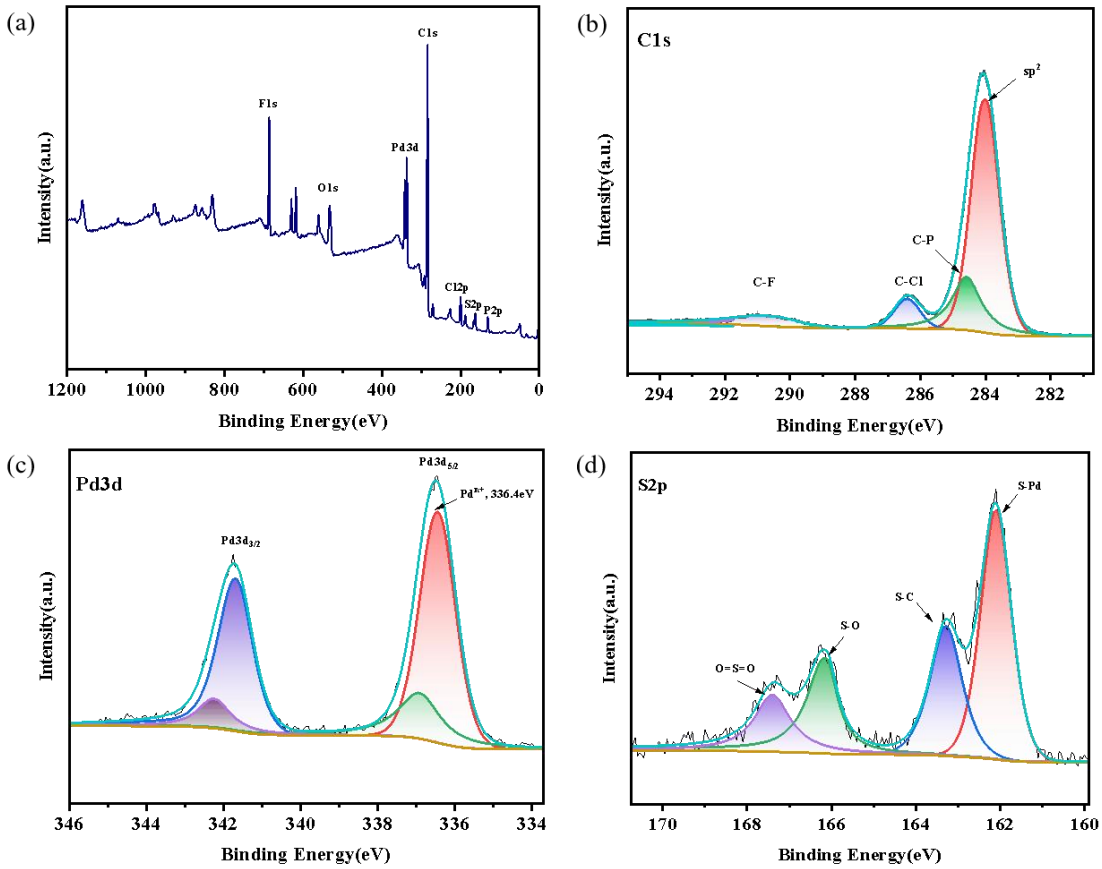

Fig. S3. (a) XPS survey spectrum of complex **5**, high-resolution (b) C 1s, (c) Pd 3d, (d) S 2p spectra of complex **5**.

For better understanding the bonding forms and valence states for complex **5**, we examined it by X-ray Photoelectron Spectroscopy (XPS). Firstly, the observed binding energies for their involved elements: Pd, C, O, S, Cl, P and F presented to be completely consistent with atoms in analogous structures and definitely manifested their existences (Fig. S3a). The high-resolution XPS spectrum for C1s in complex **5** presented four characteristic peaks at 284.00, 284.59, 286.41, and 291.57 eV (Fig. S3b), which were ascribed to the sp^2 carbon, C-P, C-Cl, and C-F, respectively. The XPS for Pd 3d in complex **5** showed two peaks at 336.40 and 341.90 eV, which were certainly assigned to Pd^{n+} $3d_{5/2}$ and Pd^{n+} $3d_{3/2}$, respectively (Fig. S3c). In addition, the high-resolution XPS spectrum for S2p presented four peaks at 162.10, 163.30, 166.15, and 167.40 eV, responding to the S-Pd, S-C, S-O, and O=S=O, respectively (Fig. S3d).

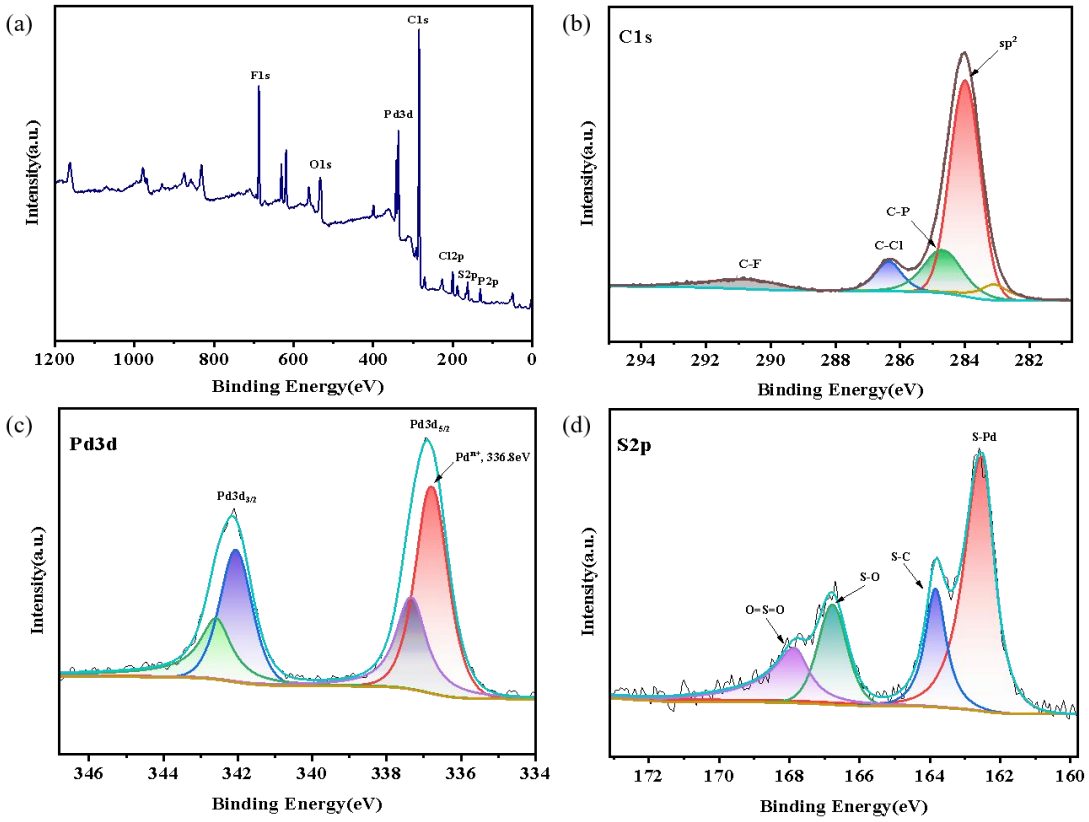

Fig. S4. (a) XPS survey spectrum of complex **6**, high-resolution (b) C 1s, (c) Pd 3d, (d) S 2p spectra of complex **6**.

For better understanding the bonding forms and valence states for complex **6**, we further examined it by X-ray Photoelectron Spectroscopy (XPS). Firstly, the observed binding energies for their involved elements: Pd, C, O, S, Cl, P and F presented to be completely consistent with atoms in analogous structures and definitely manifested their existences (Fig. S4a). For example, the high-resolution XPS spectrum for C1s in complex **6** presented four characteristic peaks at 284.00, 284.75, 286.35, and 291.40 eV (Fig. S4b), which were ascribed to the sp^2 carbon, C-P, C-Cl, and C-F, respectively. The XPS for Pd3d in complex **6** showed two peaks at 336.80 and 341.55 eV , which were certainly assigned to Pd^{n+} $3d_{5/2}$ and Pd^{n+} $3d_{3/2}$, respectively (Fig. S4c). In addition, the high-resolution XPS spectrum for S2p presented four peaks at 162.55, 163.85, 166.80, and 167.85 eV, responding to the S-Pd, S-C, S-O, and O=S=O, respectively (Fig. S4d).

5. Photochemical properties for complexes 3-6

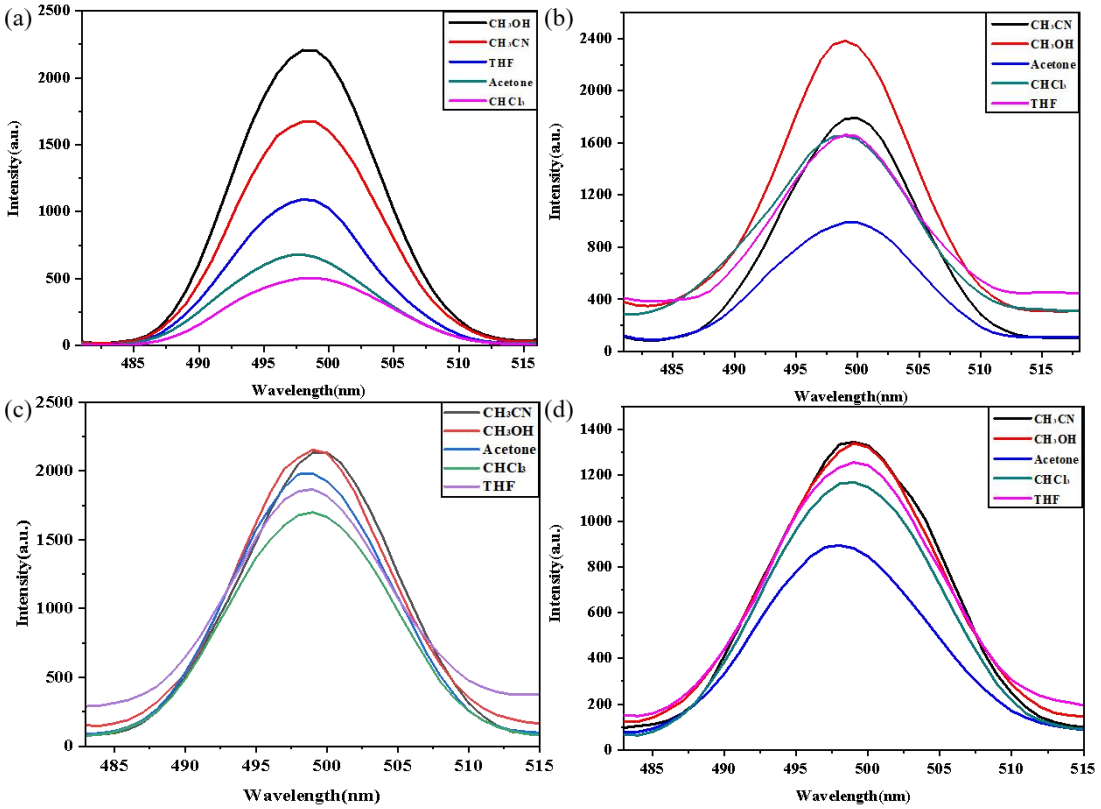

Fig. S5. Fluorescence emission of (a) complex **3** (b) complex **4**, (c) complex **5**, (d) complex **6** (λex = 250 nm) in different solvents (CH_3OH, CH_3COCH_3, $CHCl_3$, CH_3CN, THF).

It can be seen from **Fig. S5**, compared with complexes **3** and **4**, that complexes **5** and **6** were less exactly conform to the rule that the fluorescence intensity enhances with increasing solvent polarity. Part of the complexes showed fluorescence enhancement or attenuation phenomenon in certain organic solvents, possibly due to its combined interaction of solvent polarity and hydrogen bonds with the solvent, thus changing the structure and enhancing or decreasing the fluorescence intensity and the maximum absorption wavelength.

6. The HRMS and NMR for substituted aromatic silver sulfonates

HRMS of 2a

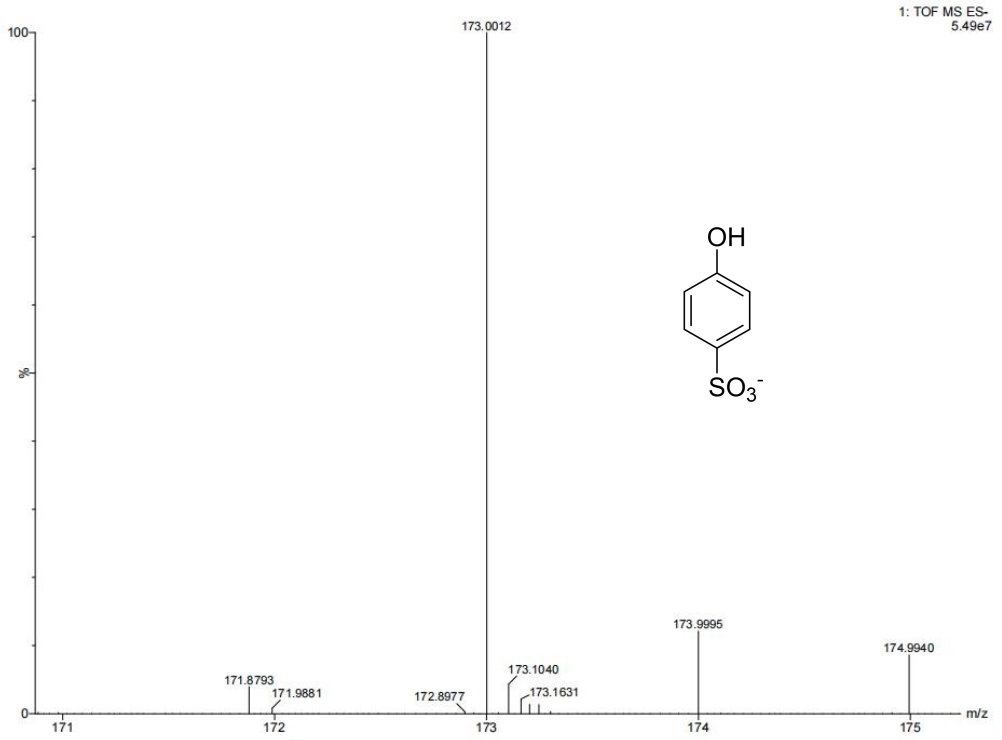

HRMS calculated for $C_6H_5O_4S^-$ 173.0014, found 173.0012.

^{1}H NMR of 2a

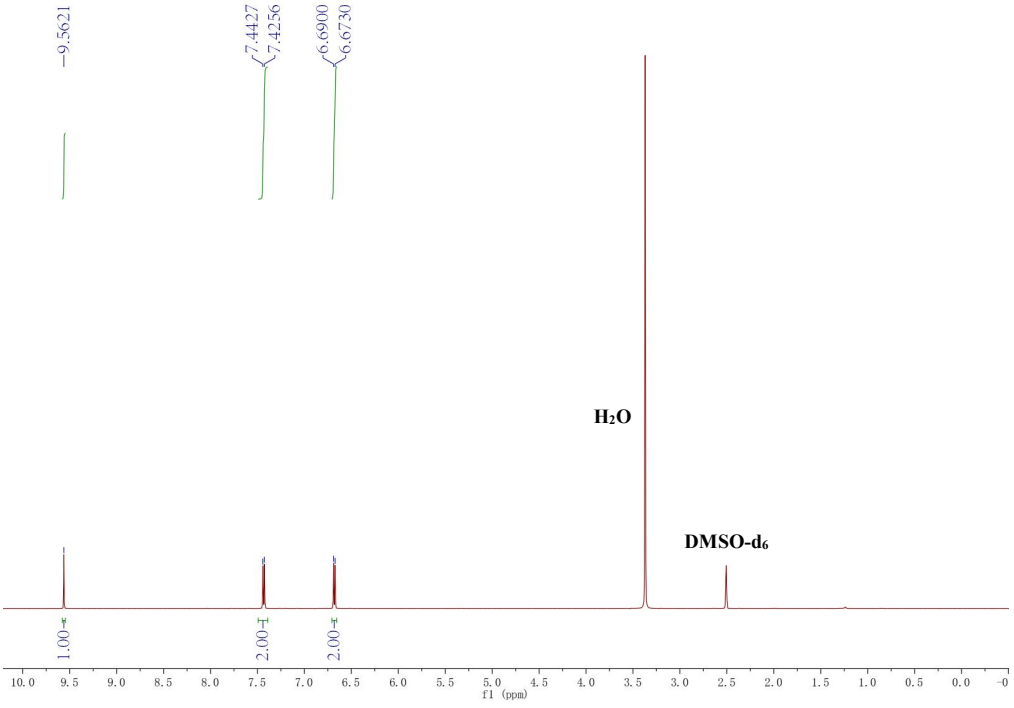

^{1}H NMR (500 MHz, DMSO-d_6) δ 9.56 (s, 1H), 7.43 (d, J = 8.5 Hz, 2H), 6.68 (d, J = 8.5 Hz, 2H).

^{13}C NMR of 2a

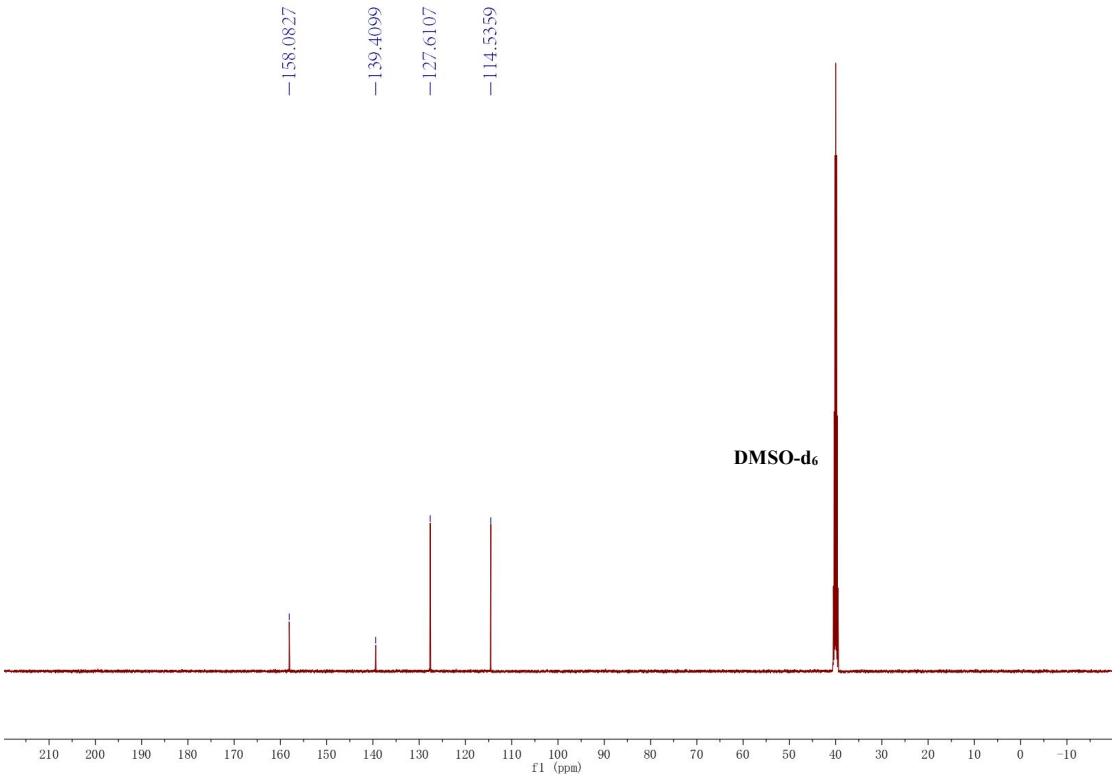

^{13}C NMR (125 MHz, DMSO-d_6) δ 158.08 (C1), 139.41 (C4), 127.61 (C2), 114.54 (C3).

HRMS of 2b

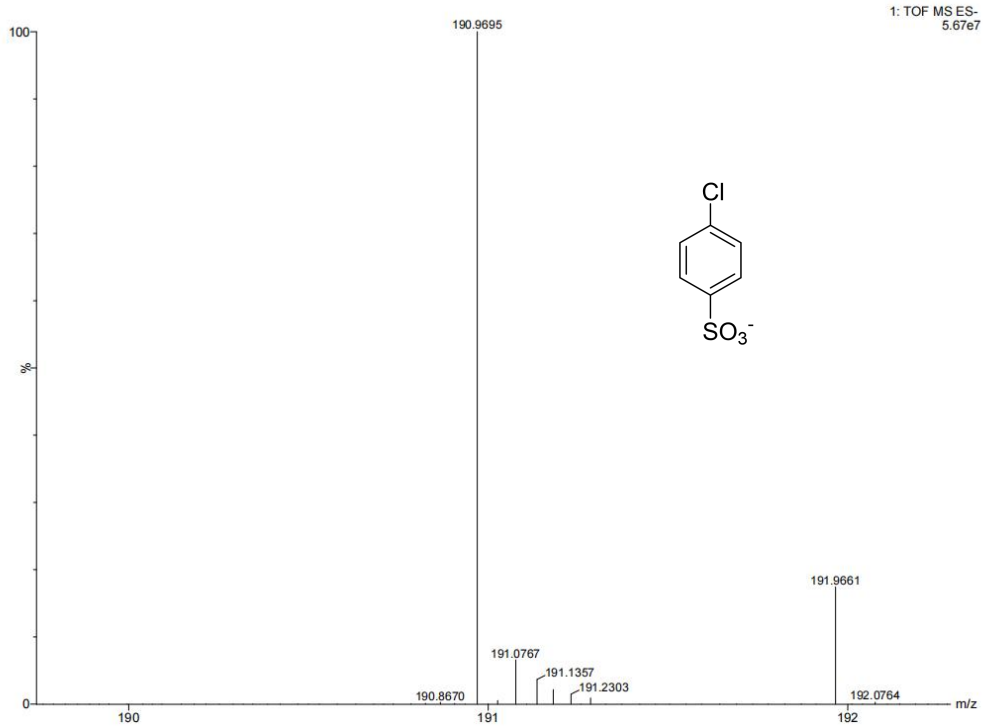

HRMS calculated for $C_6H_4ClO_3S^-$ 190.9691, found 190.9695.

^{1}H NMR of 2b

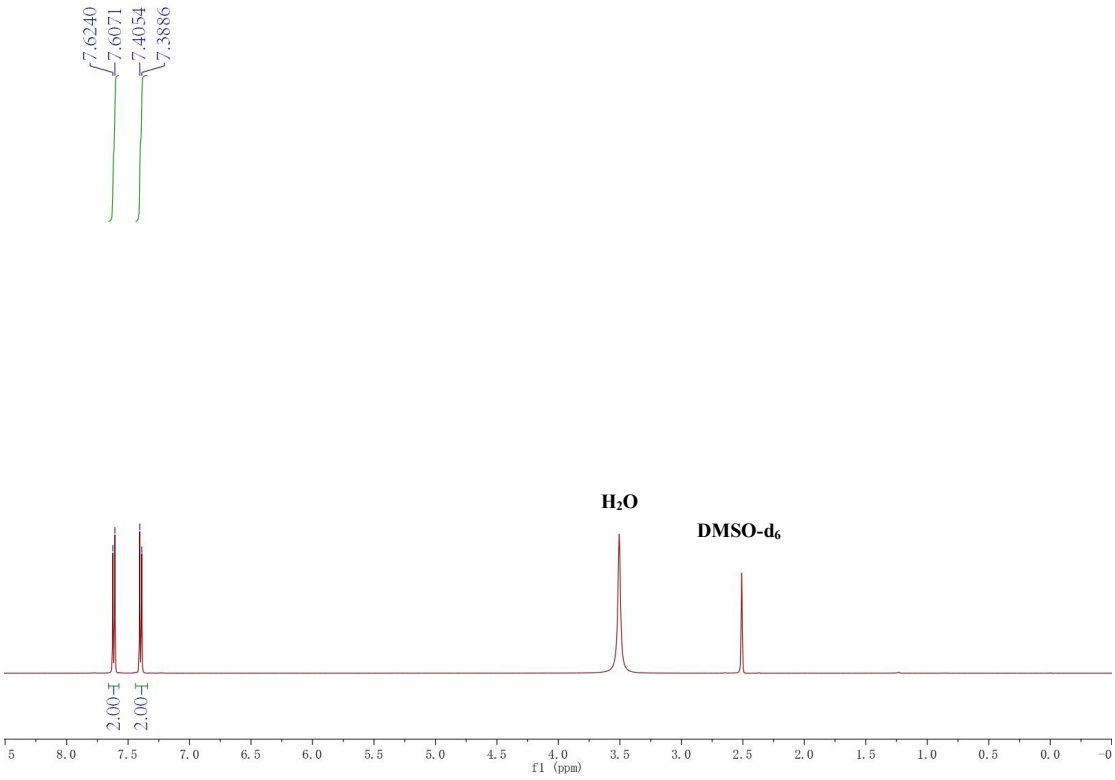

^{1}H NMR (500 MHz, DMSO-d$_6$) δ 7.62 (d, *J* = 8.5 Hz, 2H), 7.40 (d, J = 8.4 Hz, 2H).

^{13}C NMR of 2b

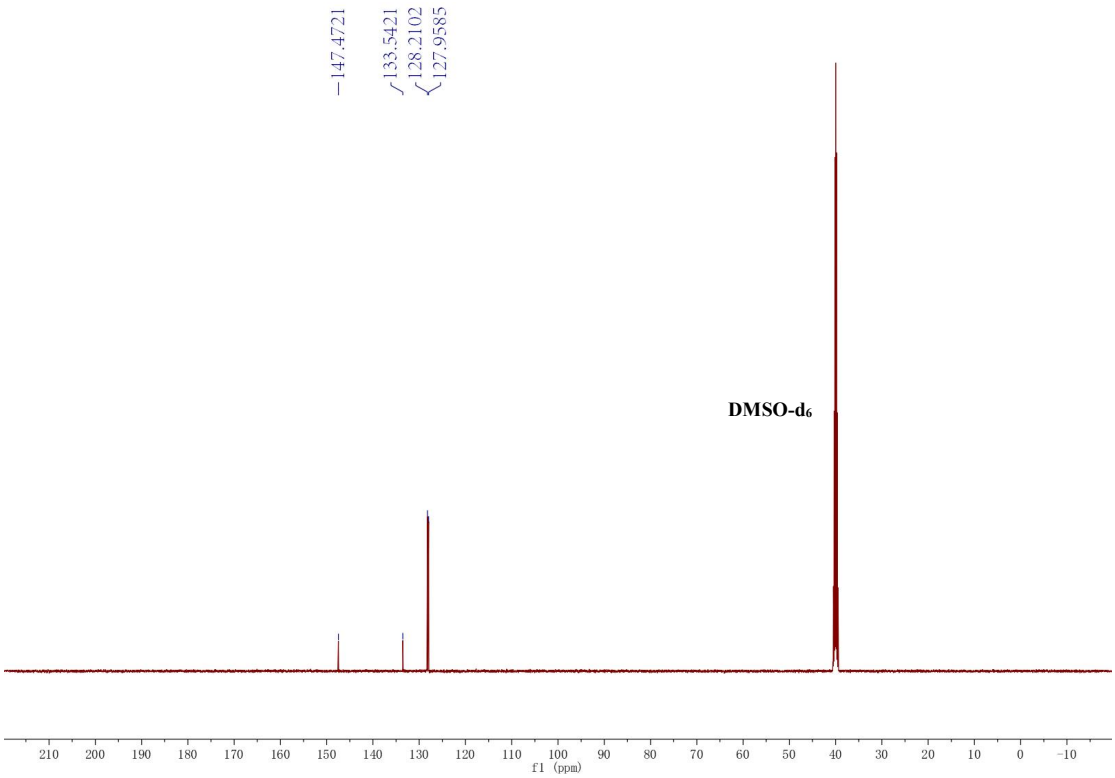

^{13}C NMR (125 MHz, DMSO-d$_6$) δ 147.47(C4), 133.54(C1), 128.21(C2), 127.96(C3).

HRMS of 2c

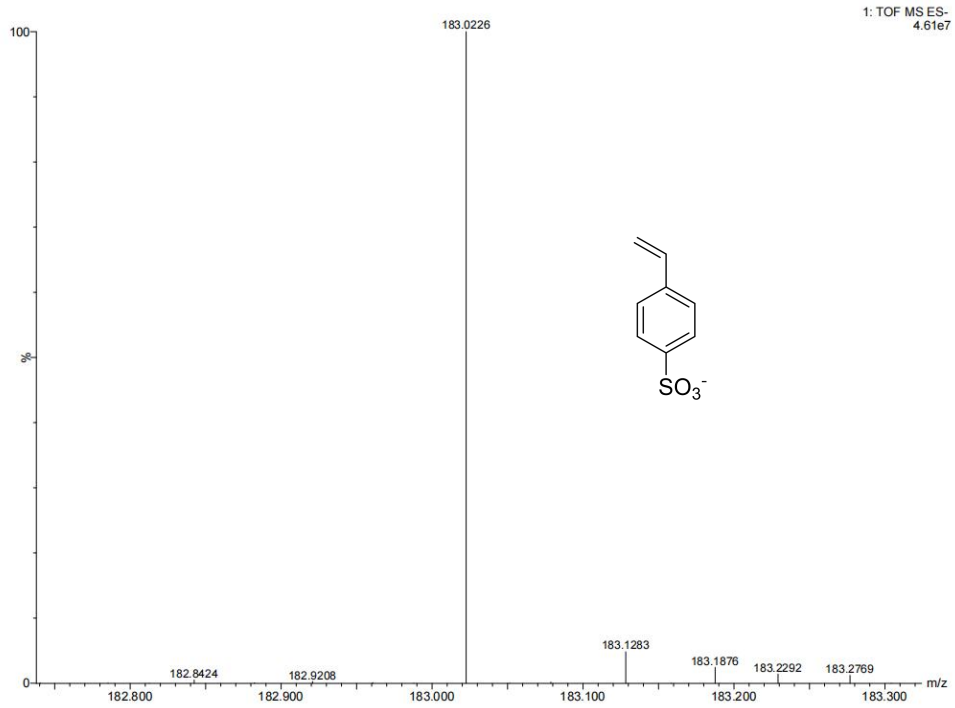

HRMS calculated for $C_8H_7O_3S^-$ 183.0221, found 183.0226.

^{1}H NMR of 2c

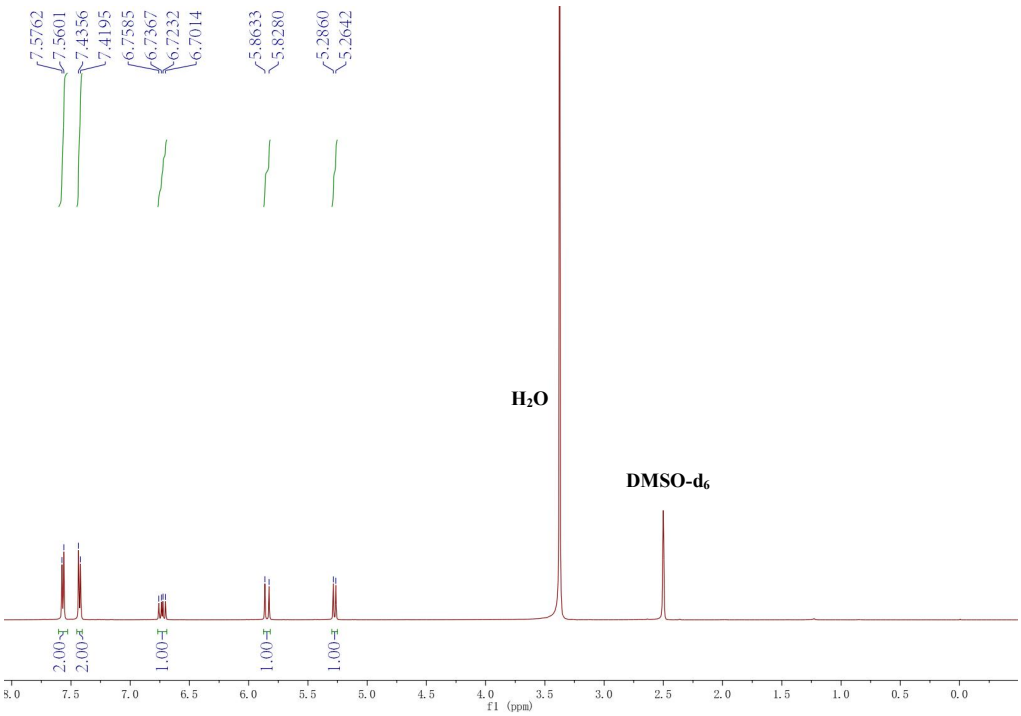

^{1}H NMR (500 MHz, DMSO-d_6) δ 7.57 (d, J = 8.1 Hz, 2H), 7.43 (d, J = 8.0 Hz, 2H), 6.73 (dd, J = 17.7, 10.9 Hz, 1H), 5.85 (d, J = 17.6 Hz, 1H), 5.28 (d, J = 10.9 Hz, 1H).

^{13}C NMR of 2c

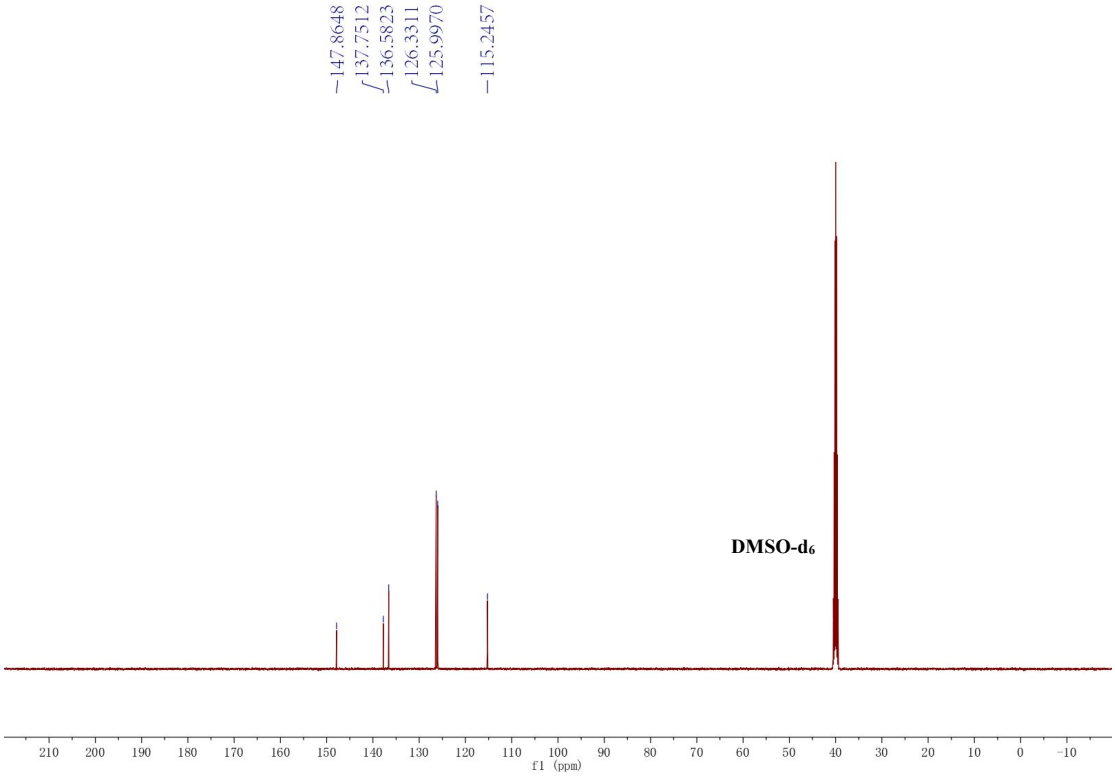

^{13}C NMR (125 MHz, DMSO-d_6) δ 147.86 (C6), 137.75 (C3), 136.58 (C2), 126.33 (C5), 126.00 (C4), 115.25 (C1).

HRMS of 2d

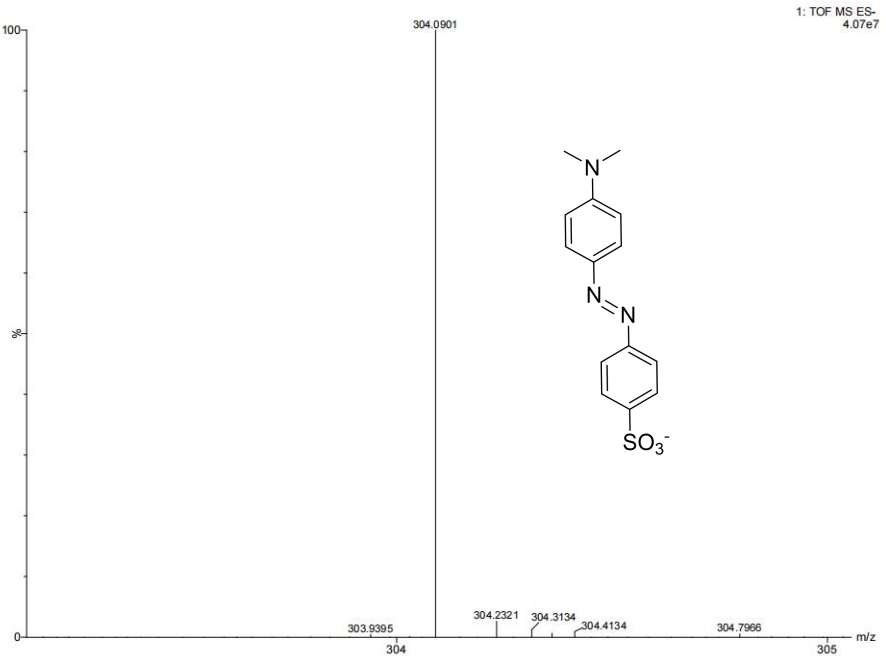

HRMS calculated for $C_{14}H_{14}N_3O_3S^-$ 304.0908, found 304.0901.

^{1}H NMR of 2d

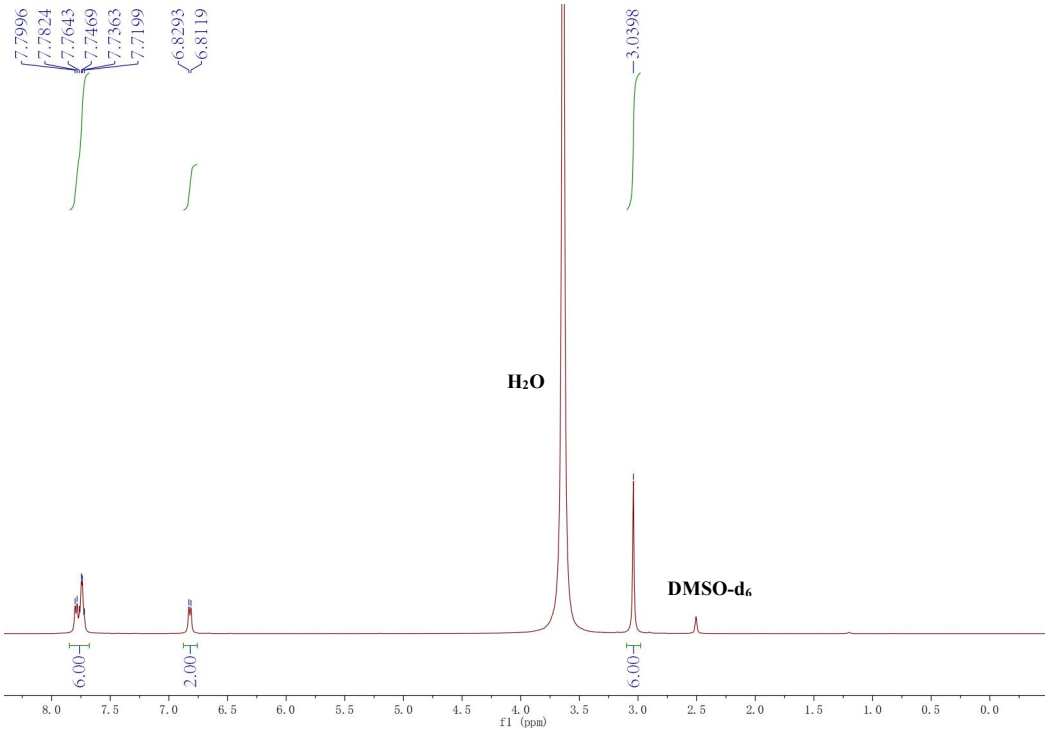

^{1}H NMR (500 MHz, DMSO-d_6) δ 7.72-7.80 (m, 6H), 6.82 (d, J = 8.7 Hz, 2H), 3.04 (s, 6H).

^{13}C NMR of 2d

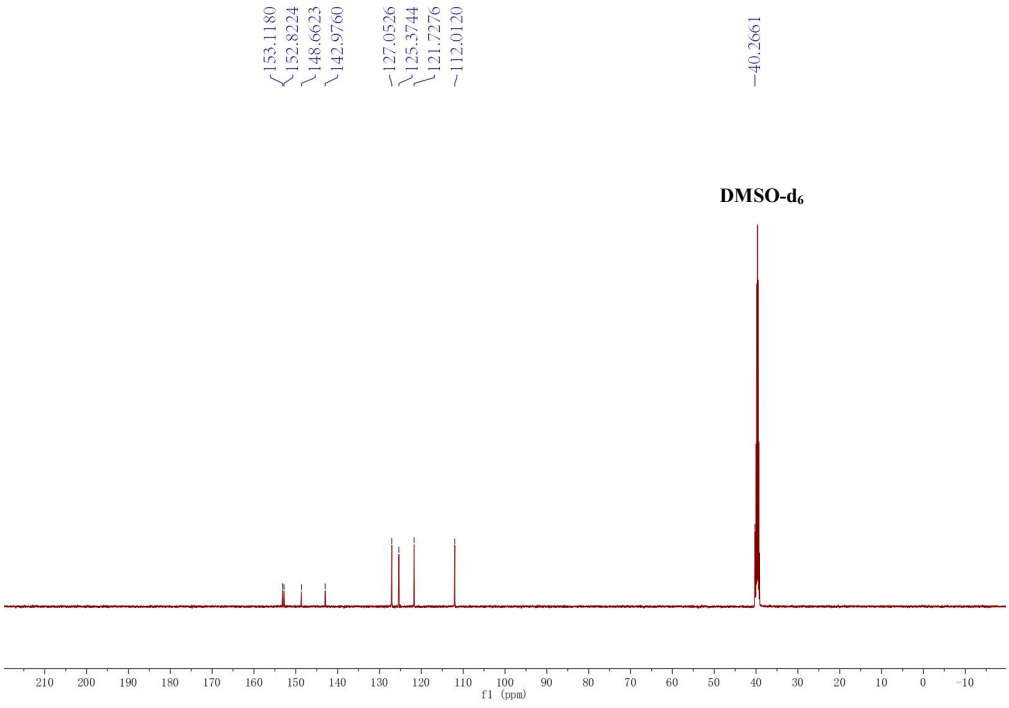

^{13}C NMR (125 MHz, DMSO-d_6) δ 153.12 (C6), 152.82 (C2), 148.66 (C9), 142.98 (C5), 127.05 (C8), 125.37 (C4), 121.73 (C7), 112.01 (C3), 40.27 (C1).

7. Copies of HRMS for complexes 4-6 and NMR for complexes 3-7

7.1 Spectra of 3 (HRMS for complex 3 is presented in the main text)

^{1}H NMR of 3

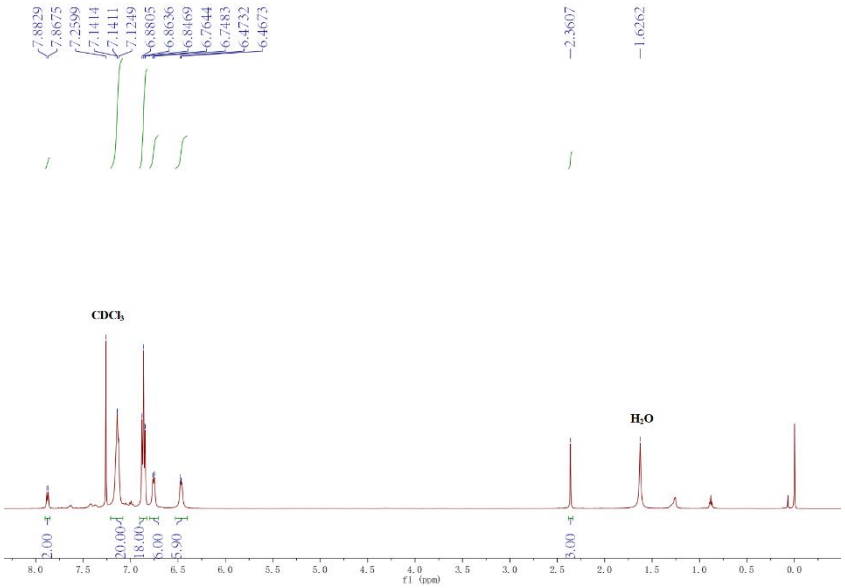

^{1}H NMR (500 MHz, $CDCl_3$) δ 7.88 (d, *J* = 7.7 Hz, 2H), 7.21-7.07 (m, 20H), 6.86 (t, *J* = 8.4 Hz, 18H), 6.76 (d, *J* = 8.0 Hz, 6H), 6.47 (s, 6H), 2.36 (s, 3H). ^{31}P NMR (202 MHz, $CDCl_3$) δ 13.41.

^{13}C NMR of 3

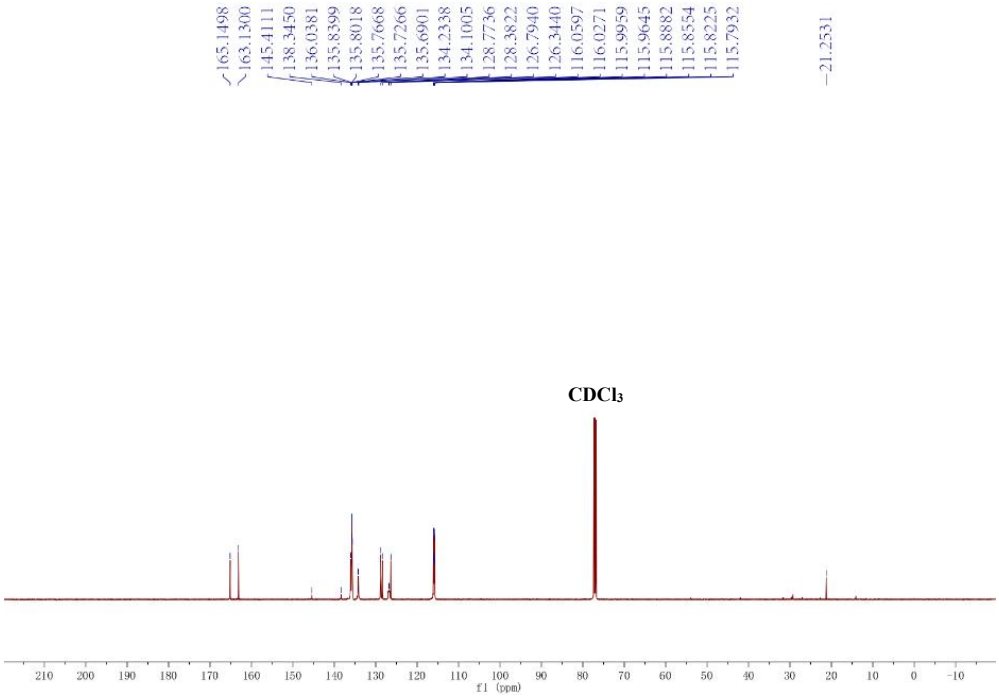

^{13}C NMR (125 MHz, $CDCl_3$) δ 164.14 (d, *J* = 254.0 Hz, C4), 145.41(C13), 138.34(C10), 136.04(C6), 135.77 (d, *J* = 9.7, 4.7 Hz, C2), 134.23(C8), 134.10(C5), 128.77(C7), 128.38(C11), 127.08-126.54 (m, C1), 126.34(C12), 115.93 (d, *J* = 21.5, 3.9 Hz, C3), 21.25(C9).

^{31}P NMR of 3

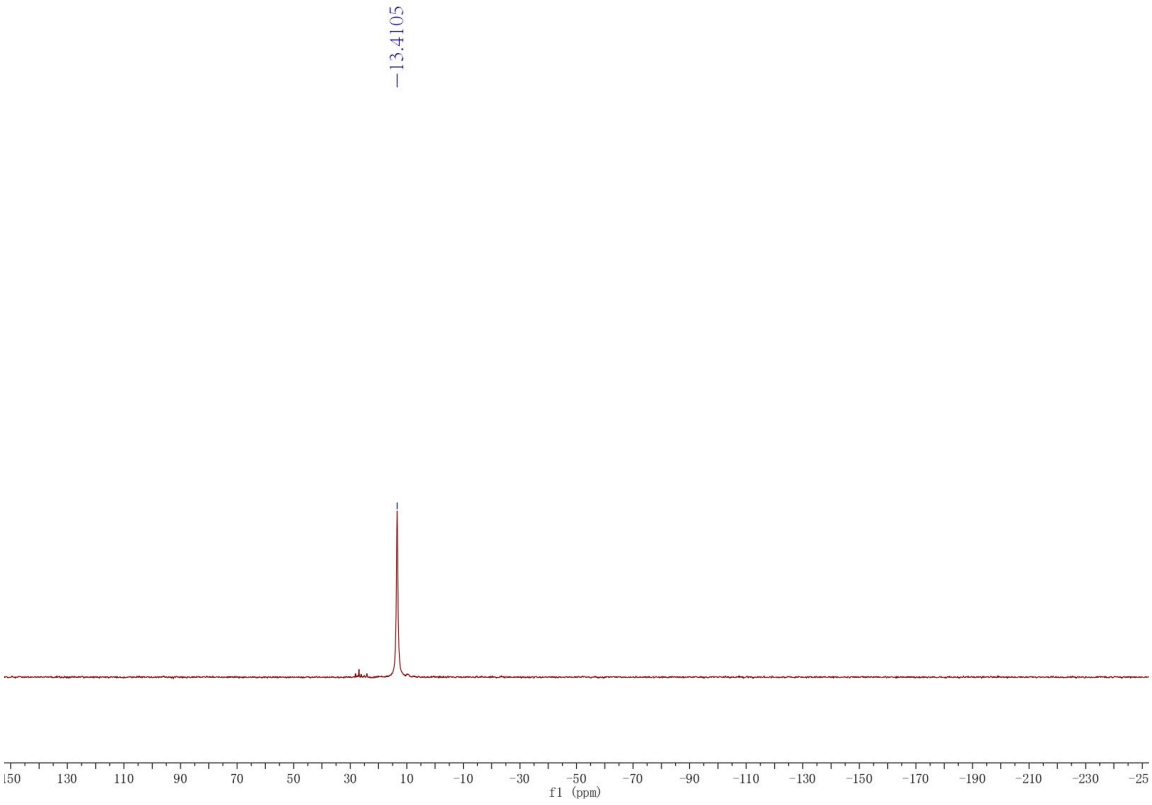

^{31}P NMR (202 MHz, $CDCl_3$) δ 13.41.

^{19}F NMR of 3

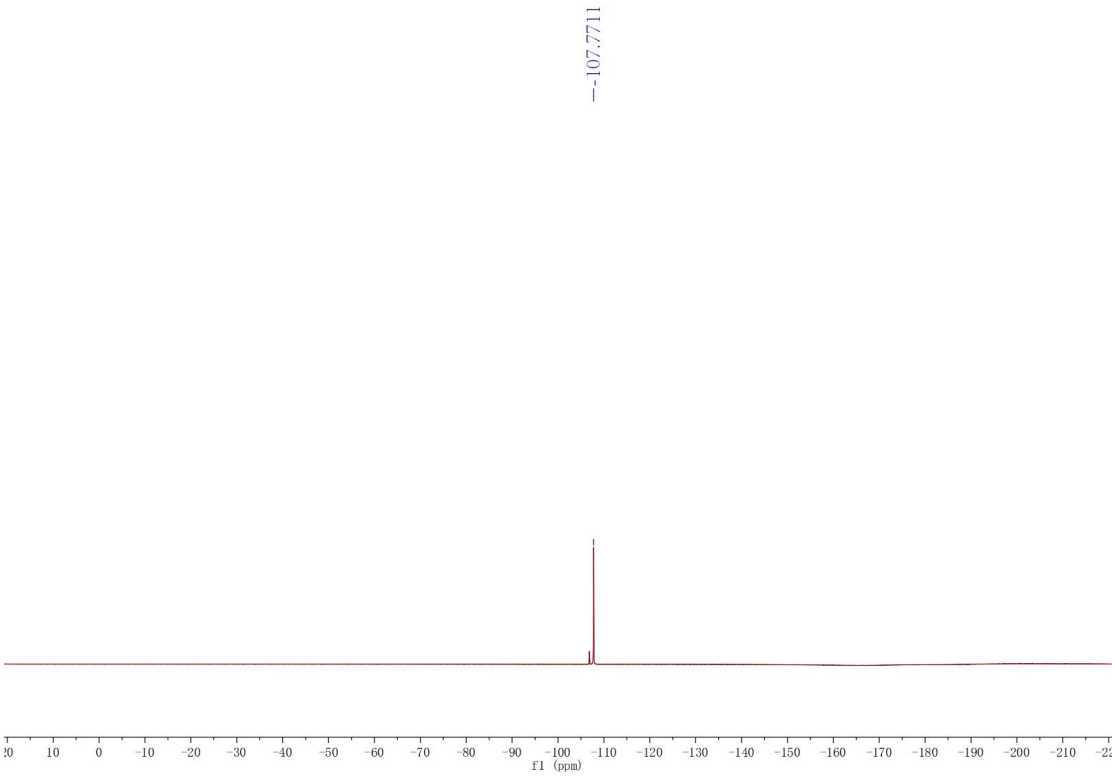

^{19}F NMR (471 MHz, $CDCl_3$) δ -107.77.

7.2 Spectra of 4

HRMS of 4

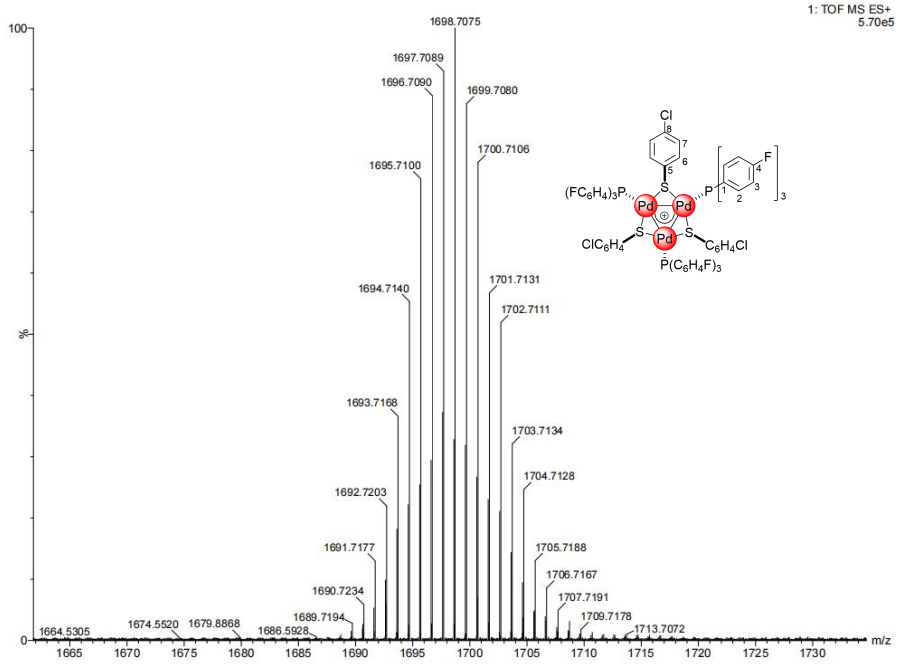

HRMS calculated for $C_{72}H_{48}P_3Pd_3S_3Cl_3F_9^+$ 1698.7048, found 1698.7072. HRMS calculated for $C_6H_5O_4S^-$ 172.9957, found 172.9959.

^{1}H NMR of 4

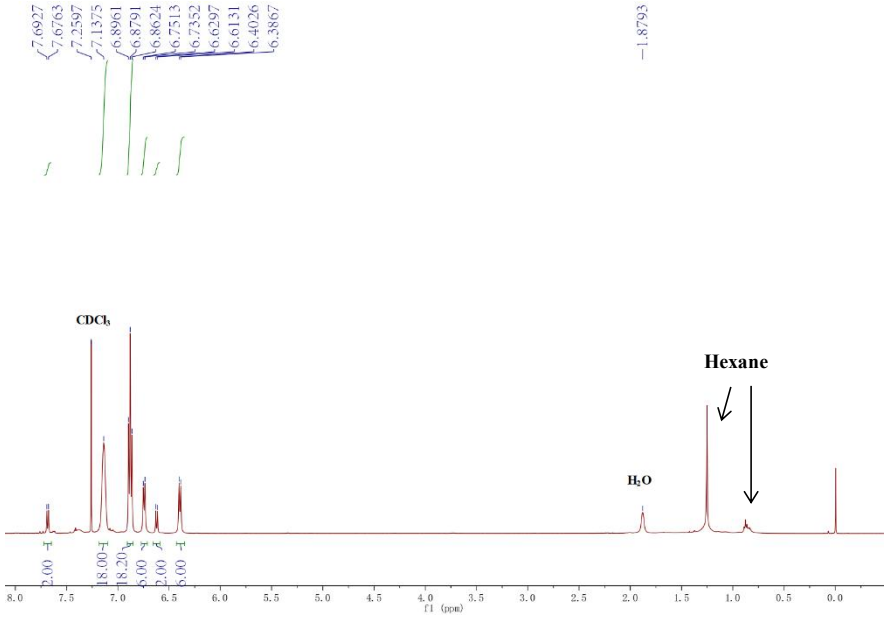

^{1}H NMR (500 MHz, $CDCl_3$) δ 7.68 (d, J = 8.2 Hz, 2H), 7.14 (s, 18H), 6.88 (t, *J* = 8.4 Hz, 18H), 6.74 (d, *J* = 8.0 Hz, 6H), 6.62 (d, *J* = 8.3 Hz, 2H), 6.39 (d, *J* = 8.0 Hz, 6H).

^{13}C NMR of 4

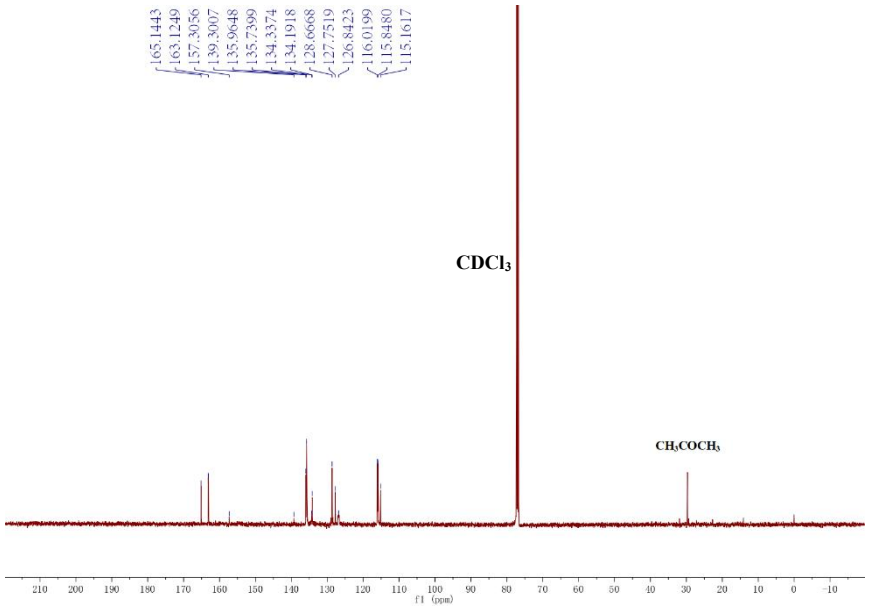

^{13}C NMR (125 MHz, $CDCl_3$) δ 164.13 (d, *J* = 254.0 Hz, C4), 157.31 (C9), 139.30 (C12), 135.96 (C6), 135.74 (d, *J* = 9.5, 5.0 Hz, C2), 134.34 (C8), 134.19 (C5), 128.67 (C7), 127.75 (C10), 127.09-126.57 (m, C1), 115.93 (d, *J* = 21.4, 3.9 Hz, C3), 115.16 (C11).

^{31}P NMR of 4

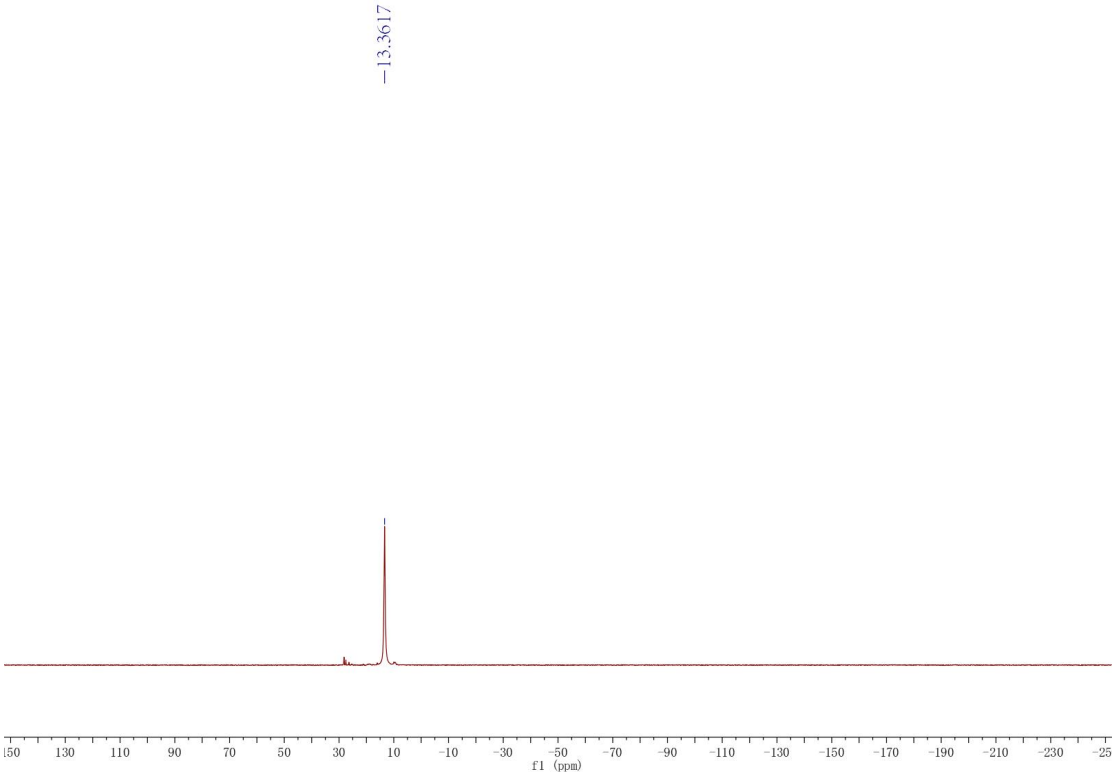

^{31}P NMR (202 MHz, $CDCl_3$) δ 13.36.

^{19}F NMR of 4

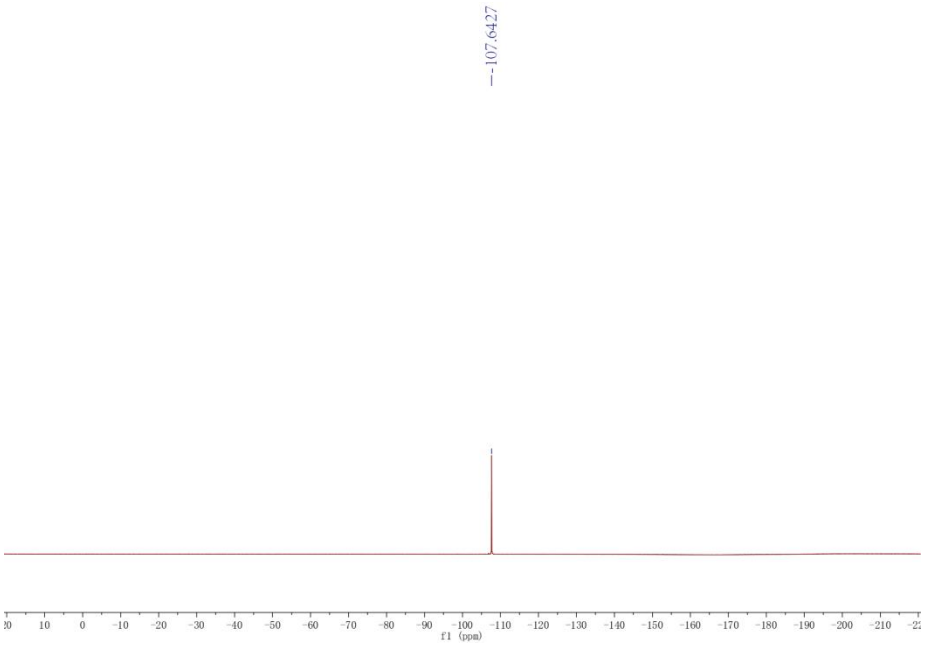

^{19}F NMR (471 MHz, $CDCl_3$) δ -107.64.

7.3 Spectra of 5

HRMS of 5

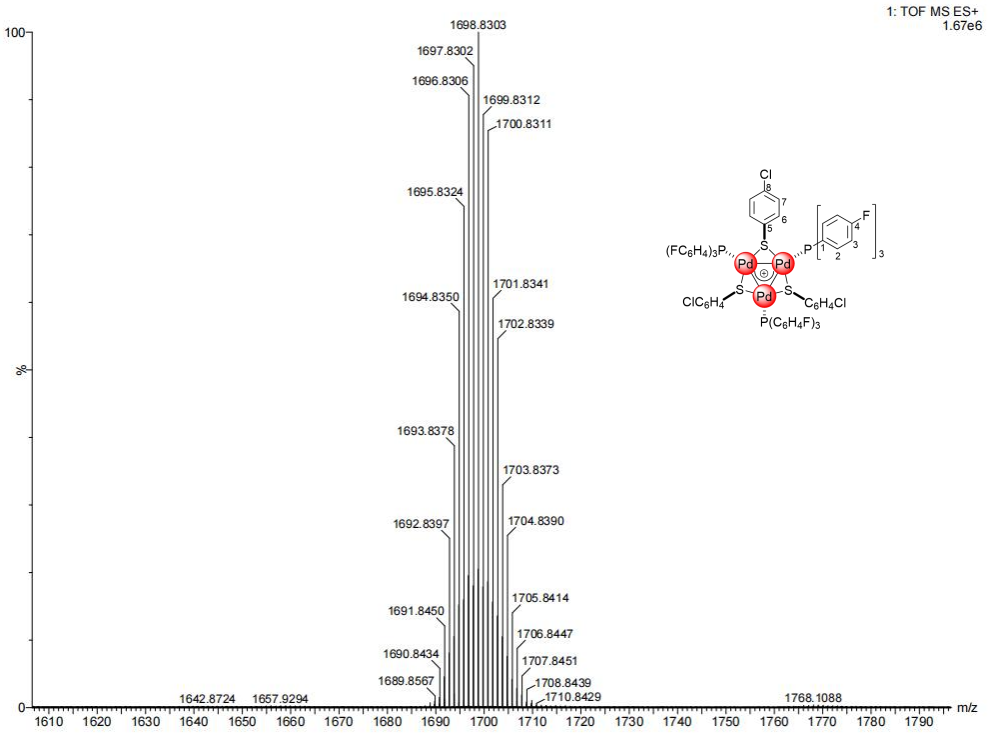

HRMS calculated for $C_{72}H_{48}P_3Pd_3S_3Cl_3F_9^+$ 1698.8362, found 1698.8303. HRMS calculated for $C_6H_4ClO_3S^-$ 190.9625, found 190.9623.

[1]H NMR of 5

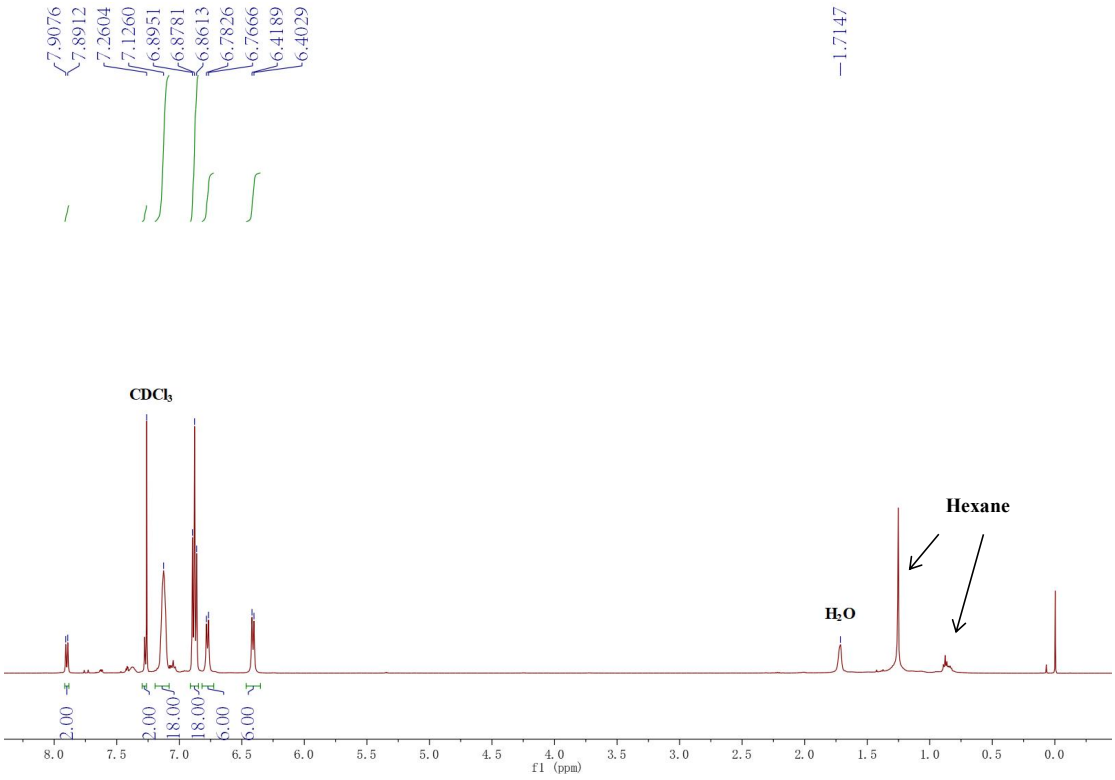

^{1}H NMR (500 MHz, $CDCl_3$) δ 7.90 (d, *J* = 8.2 Hz, 2H), 7.28 (s, 2H), 7.13 (s, 18H), 6.88 (t, *J* = 8.4 Hz, 18H), 6.77 (d, *J* = 8.0 Hz, 6H), 6.41 (d, *J* = 8.0 Hz, 6H).

[13]C NMR of 5

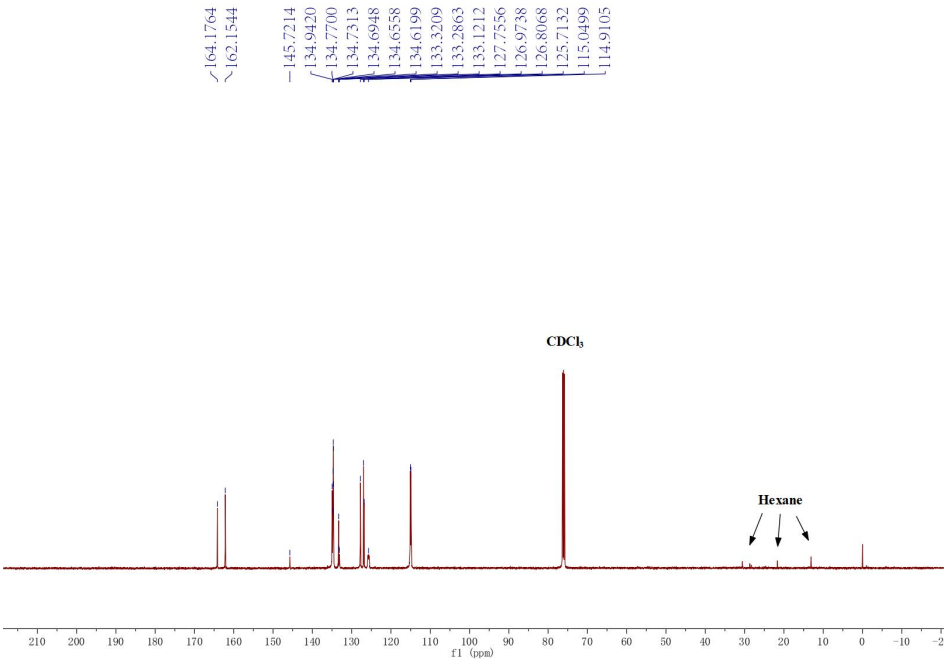

^{13}C NMR (125 MHz, $CDCl_3$) δ 163.17 (d, *J* = 254.3 Hz, C4), 145.72 (C12), 134.94 (C6), 134.69 (d, *J* = 9.4, 4.7 Hz, C2), 133.32 (C8), 133.29 (C5), 133.12 (C9), 127.76 (C7), 126.97 (C10), 126.81 (C11), 125.76 (dr, *J* = 34.5, 12.9 Hz, C1), 114.98 (d, *J* = 21.8, 4.1 Hz, C3).

^{31}P NMR of 5

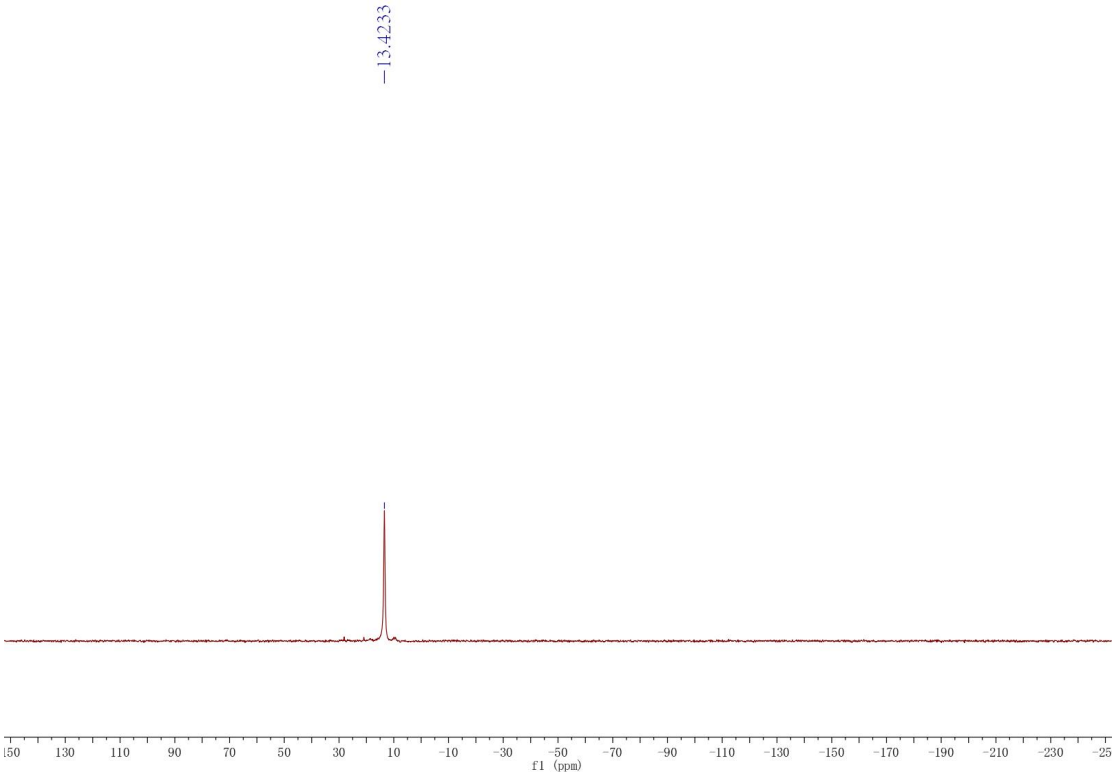

^{31}P NMR (202 MHz, $CDCl_3$) δ 13.42.

^{19}F NMR of 5

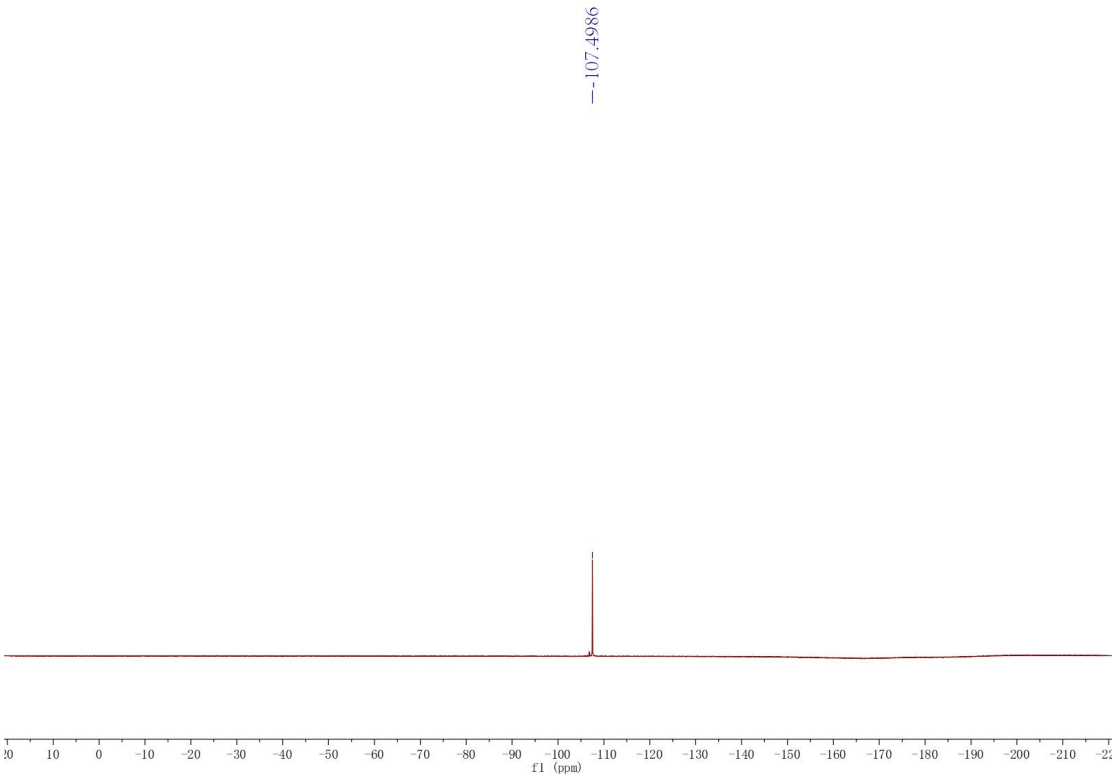

^{19}F NMR (471 MHz, $CDCl_3$) δ -107.50.

7.4 Spectra of 6

HRMS of 6

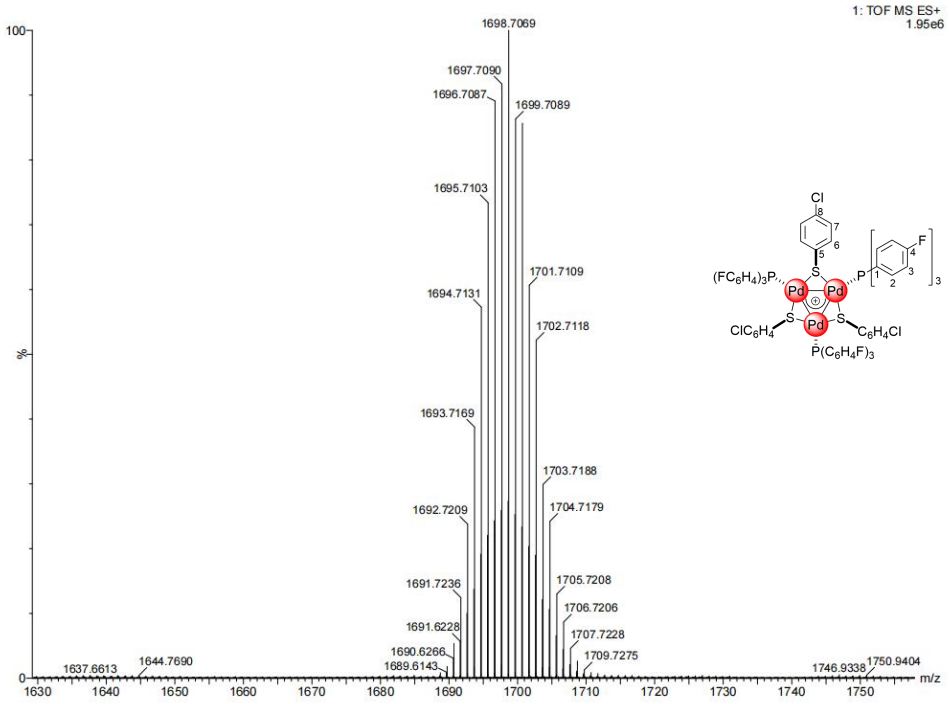

HRMS calculated for $C_{72}H_{48}P_3Pd_3S_3Cl_3F_9^+$ 1698.7048, found 1698.7067. HRMS calculated for $C_8H_7O_3S^-$ 183.0161. found 183.0165.

^{1}H NMR of 6

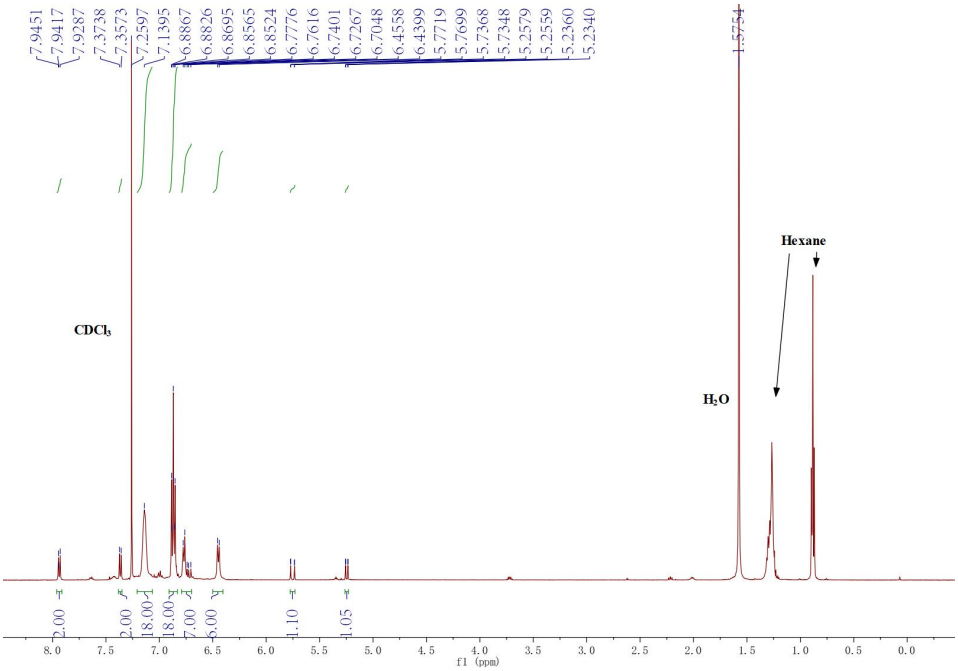

^{1}H NMR (500 MHz, $CDCl_3$) δ 7.94 (d, J = 8.2 Hz, 2H), 7.37 (d, J = 8.2 Hz, 2H), 7.14 (s, 18H), 6.87 (t, J = 8.6 Hz, 18H), 6.79-6.70 (m, 7H), 6.45 (d, J = 8.0 Hz, 6H), 5.75 (dd, J = 17.5, 1.0 Hz, 1H), 5.25 (dd, J = 11.0, 1.0 Hz, 1H).

^{13}C NMR of 6

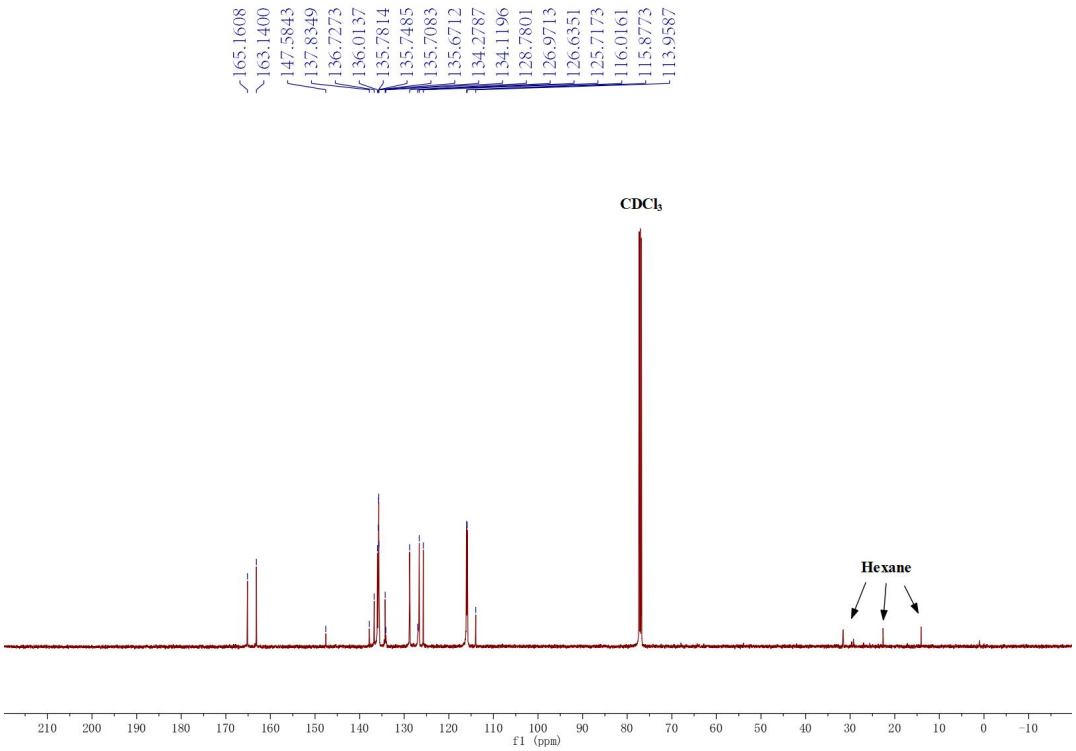

^{13}C NMR (125 MHz, $CDCl_3$) δ 164.15 (d, *J* = 254.2 Hz, C4), 147.58 (C14), 137.83 (C11), 136.73 (C10), 136.01 (C6), 135.92-135.60 (m, C2), 134.28 (C8), 134.12 (C5), 128.78 (C7), 126.97 (C1), 126.64 (C13), 125.72 (C12), 115.95 (d, C3), 113.96 (C9).

^{31}P NMR of 6

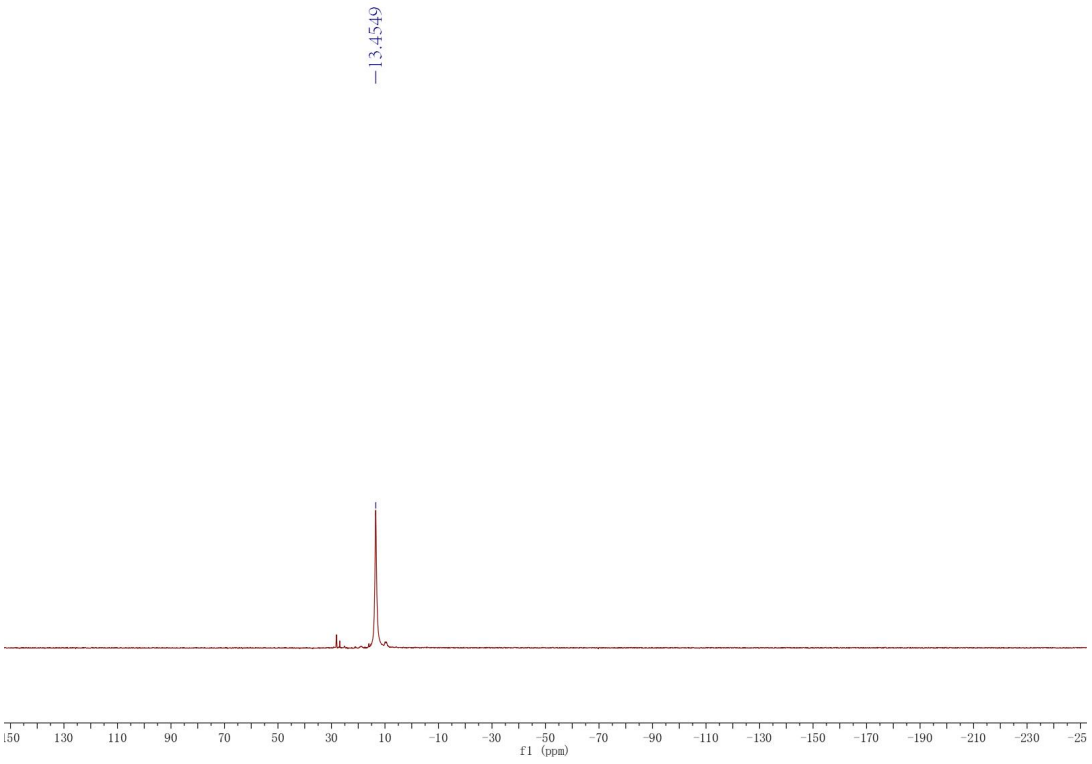

^{31}P NMR (202 MHz, $CDCl_3$) δ 13.45.

^{19}F NMR of 6

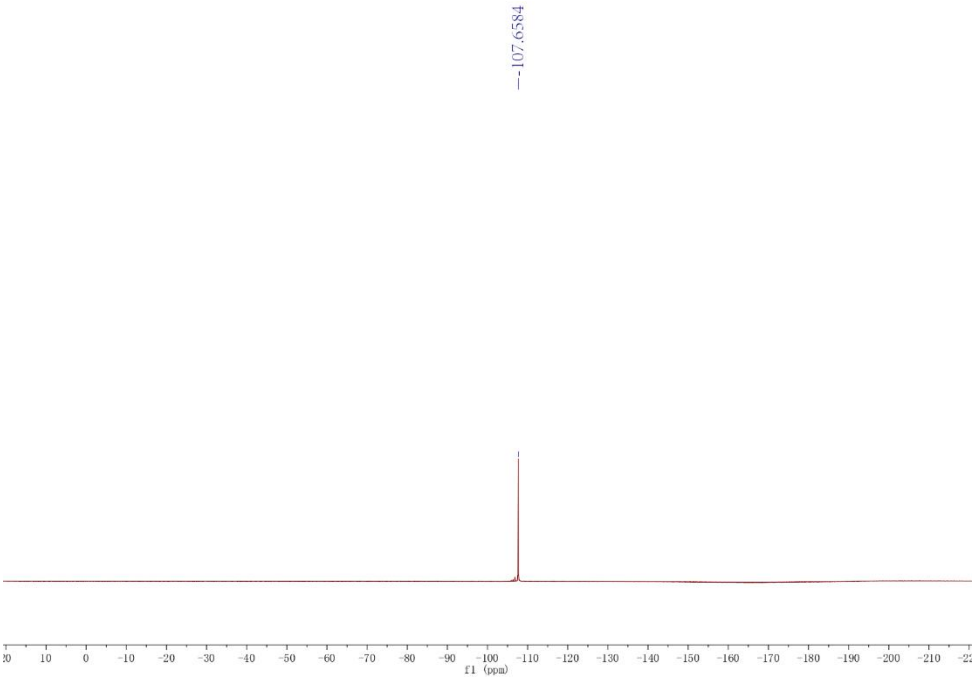

^{19}F NMR (471 MHz, $CDCl_3$) δ -107.66.

7.5 Spectra of 7

HRMS of 7

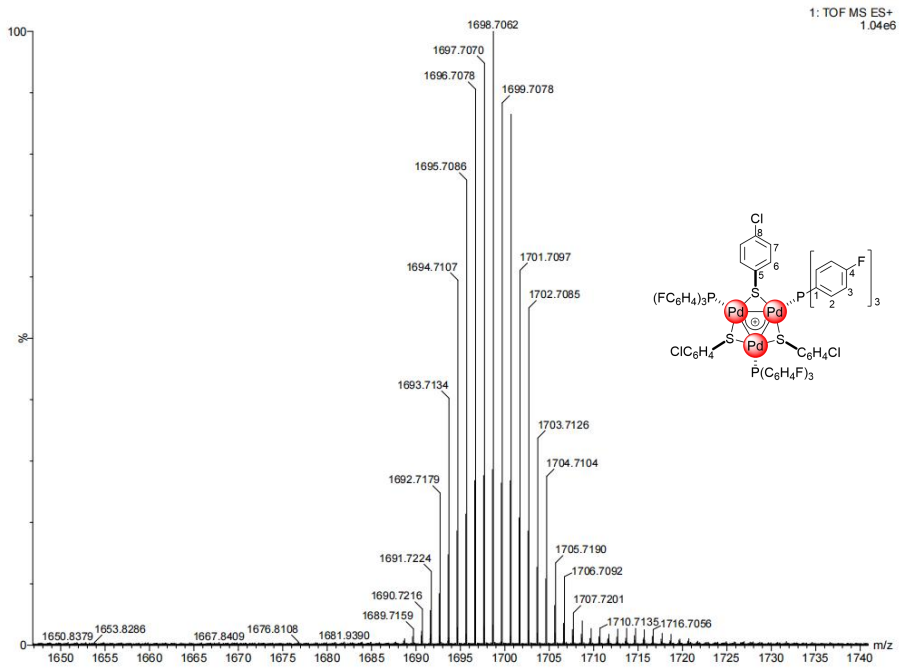

HRMS calculated for $C_{72}H_{48}P_3Pd_3S_3Cl_3F_9^+$ 1698.7048, found 1698.7059. HRMS calculated for $C_{14}H_{14}N_3O_3S^-$ 304.0801, found 304.0802.

[1]H NMR of 7

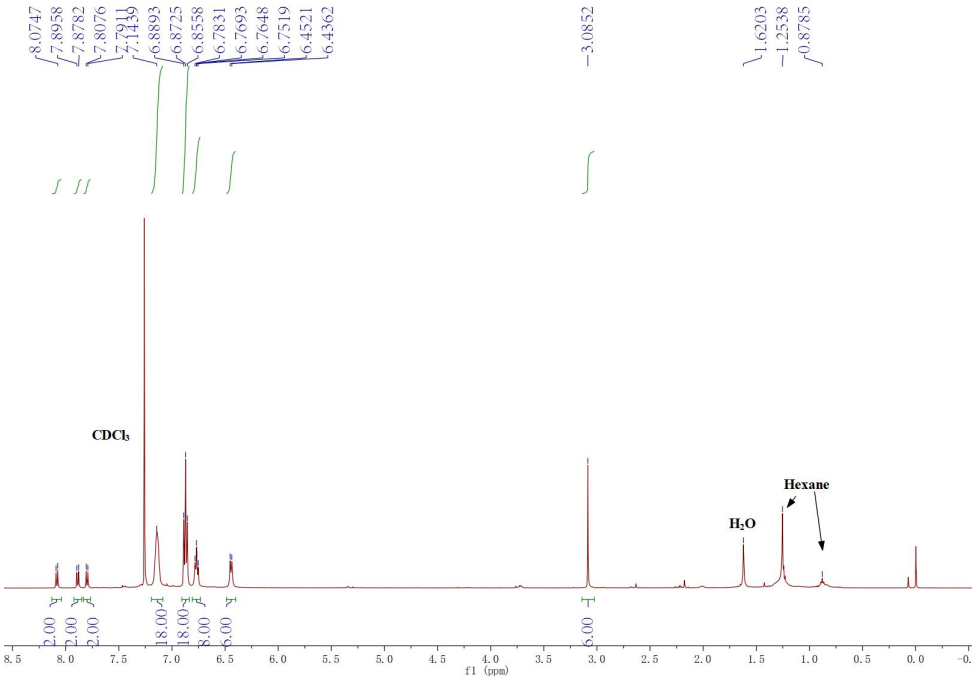

[1]H NMR (500 MHz, $CDCl_3$) δ 8.08 (d, *J* = 8.3 Hz, 2H), 7.89 (d, *J* = 8.8 Hz, 2H), 7.80 (d, *J* = 8.2 Hz, 2H), 7.14 (s, 18H), 6.87 (t, *J* = 8.4 Hz, 18H), 6.77 (b, 8H), 6.44 (d, *J* = 8.0 Hz, 6H), 3.09 (s, 6H).

[13]C NMR of 7

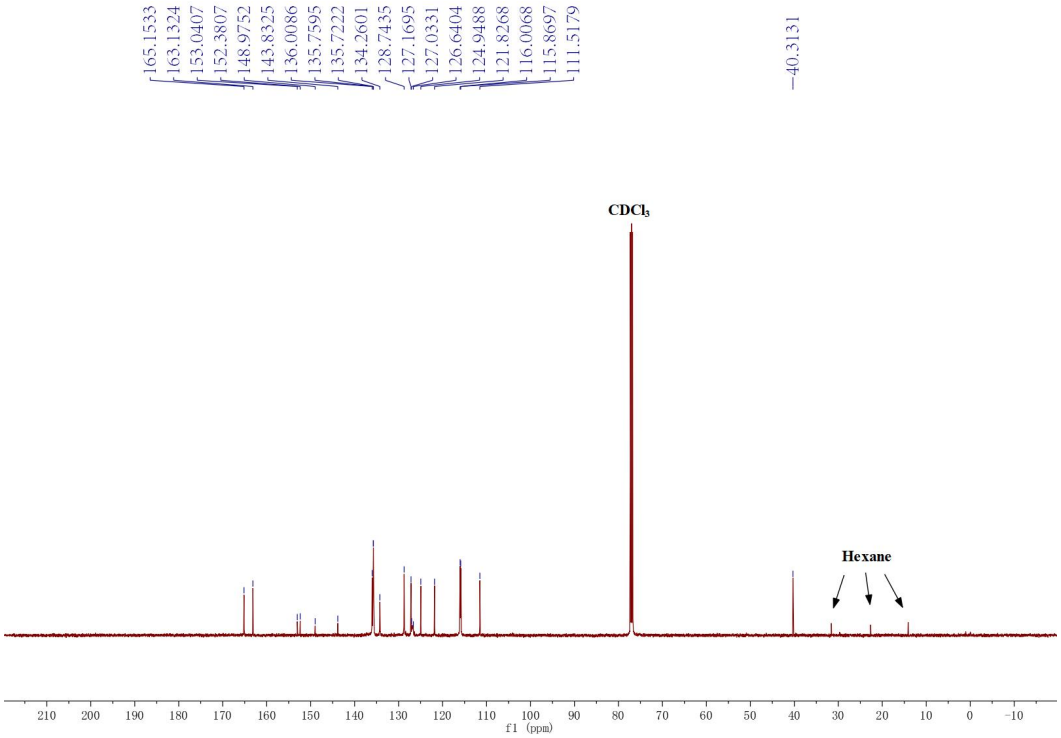

[13]C NMR (125 MHz, $CDCl_3$) δ 164.14 (d, *J* = 254.2 Hz, C4), 153.04 (C14), 152.38 (C10), 148.98 (C17), 143.83 (C13), 136.01 (C6), 135.74 (d, *J* = 4.7 Hz, C2), 134.26 (C5), 128.74 (C7), 127.17 (C16), 127.17-126.57 (m, C1), 124.95 (C12), 121.83 (C15), 115.94 (d, *J* = 17.3 Hz, C3), 111.52(C11), 40.31(C9).

^{31}P NMR of 7

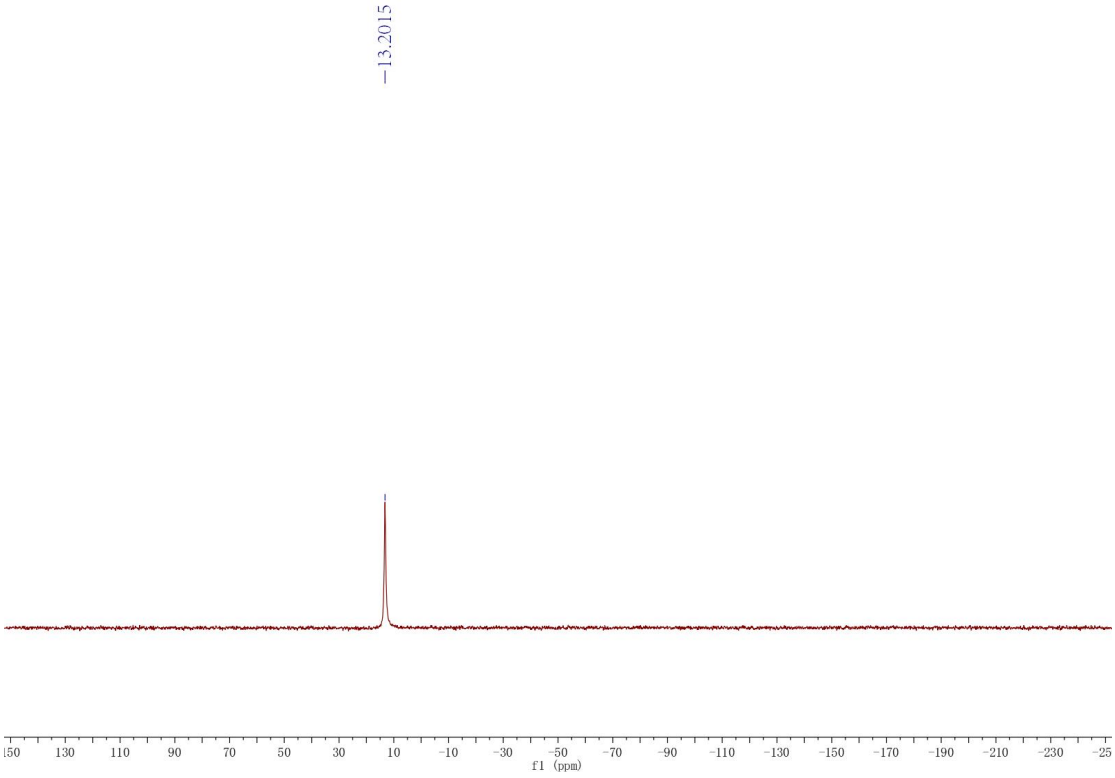

^{31}P NMR (202 MHz, $CDCl_3$) δ 13.20.

^{19}F NMR of 7

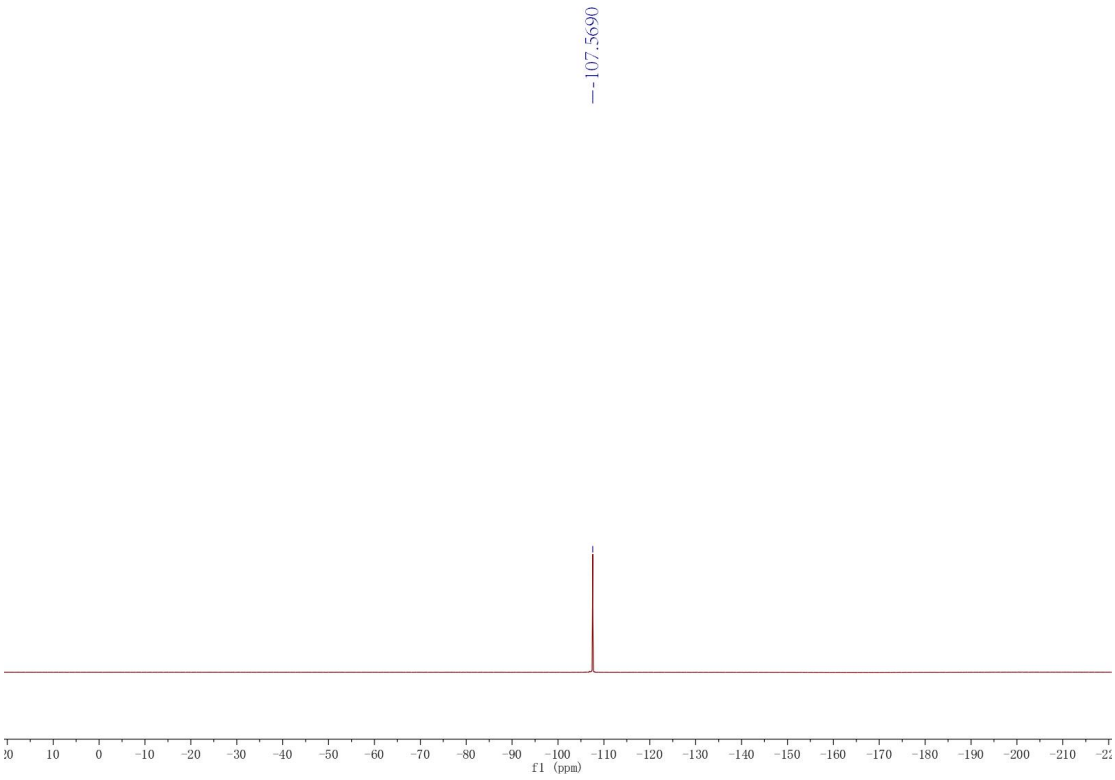

^{19}F NMR (471 MHz, $CDCl_3$) δ -107.57.

8. The crystallography data for complex 7

Table S1. Crystal data and structure refinement for complex **7** (CCDC 2270588).

Identification code	complex **7**
Empirical formula	$C_{86}H_{62}Cl_3F_9N_3O_3P_3Pd_3S_4$
Formula weight	2003.08
Temperature	293(2) K
Wavelength	1.54184 Å
Crystal system, space group	Monoclinic， P2(1)/c
Unit cell dimensions	a = 14.6261(10) Å alpha = 90 deg. b = 30.7775(17) Å beta = 106.865(7) deg. c = 20.8709(14) Å gamma = 90 deg.
Volume	8991.1(10) $Å^3$
Z, Calculated density	4， 1.480 Mg/m^3
Absorption coefficient	7.542 mm^{-1}
F(000)	4008
Crystal size	0.080×0.080×0.070 mm
Theta range for data collection	2.637 to 67.249 deg.
Limiting indices	-17<=h<=14, -27<=k<=36, -16<=l<=24
Reflections collected / unique	32651 / 16063 [R(int) = 0.0703]
Completeness to theta = 67.684	0.988
Absorption correction	Semi-empirical from equivalents
Max. and min. transmission	1.00000 and 0.63046
Refinement method	Full-matrix least-squares on F^2
Data / restraints / parameters	16063 / 2892 / 1029
Goodness-of-fit on F^2	0.938
Final R indices [I>2sigma(I)]	R1 = 0.0671, wR2 = 0.1596
R indices (all data)	R1 = 0.1381, wR2 = 0.2062
Extinction coefficient	n/a
Largest diff. peak and hole	0.992 and -0.791 e. $Å^{-3}$

Table S2. Bond lengths[Å] and angles [°] for complex **7**.	
Pd(1)-P(1)	2.273(2)
Pd(1)-S(3)	2.281(3)
Pd(1)-S(1)	2.283(2)
Pd(1)-Pd(3)	2.8458(10)
Pd(1)-Pd(2)	2.8577(9)
Pd(2)-S(2)	2.269(2)
Pd(2)-P(2)	2.288(3)
Pd(2)-S(3)	2.292(2)
Pd(2)-Pd(3)	2.8996(10)
Pd(3)-S(2)	2.267(2)
Pd(3)-S(1)	2.270(2)
Pd(3)-P(3)	2.282(3)
S(1)-C(1)	1.774(9)
S(2)-C(13)	1.771(10)
S(3)-C(7)	1.781(10)
S(4)-O(3)	1.432(8)
S(4)-O(2)	1.443(7)
S(4)-O(1)	1.451(8)
S(4)-C(73)	1.774(10)
Cl(1)-C(10)	1.755(10)
Cl(2)-C(4)	1.757(11)
Cl(3)-C(16)	1.728(11)
P(1)-C(25)	1.799(9)
P(1)-C(19)	1.821(10)
P(1)-C(31)	1.829(10)
P(2)-C(49)	1.804(10)
P(2)-C(37)	1.813(12)
P(2)-C(43)	1.816(10)

P(3)-C(61)	1.799(11)
P(3)-C(55)	1.806(11)
P(3)-C(67)	1.830(11)
F(1)-C(22)	1.361(13)
F(2)-C(28)	1.349(12)
F(3)-C(34)	1.365(13)
F(4)-C(40)	1.399(17)
F(5)-C(46)	1.373(12)
F(6)-C(52)	1.370(13)
F(7)-C(58)	1.366(14)
F(8)-C(64)	1.373(14)
F(9)-C(70)	1.399(15)
N(1)-C(82)	1.410(19)
N(1)-C(86)	1.44(2)
N(1)-C(85)	1.49(2)
N(2)-N(3)	1.260(15)
N(2)-C(76)	1.479(15)
N(3)-C(79)	1.525(18)

P(1)-Pd(1)-S(3)	95.41(9)
P(1)-Pd(1)-S(1)	100.90(9)
S(3)-Pd(1)-S(1)	163.55(9)
P(1)-Pd(1)-Pd(3)	152.01(7)
S(3)-Pd(1)-Pd(3)	112.57(6)
S(1)-Pd(1)-Pd(3)	51.11(6)
P(1)-Pd(1)-Pd(2)	146.77(7)
S(3)-Pd(1)-Pd(2)	51.49(6)
S(1)-Pd(1)-Pd(2)	112.09(6)
Pd(3)-Pd(1)-Pd(2)	61.11(2)
S(2)-Pd(2)-P(2)	99.40(9)

S(2)-Pd(2)-S(3)	159.92(9)
P(2)-Pd(2)-S(3)	100.13(9)
S(2)-Pd(2)-Pd(1)	109.38(7)
P(2)-Pd(2)-Pd(1)	151.21(7)
S(3)-Pd(2)-Pd(1)	51.15(6)
S(2)-Pd(2)-Pd(3)	50.23(6)
P(2)-Pd(2)-Pd(3)	149.52(7)
S(3)-Pd(2)-Pd(3)	110.35(7)
Pd(1)-Pd(2)-Pd(3)	59.24(2)
S(2)-Pd(3)-S(1)	161.32(9)
S(2)-Pd(3)-P(3)	97.26(10)
S(1)-Pd(3)-P(3)	101.40(9)
S(2)-Pd(3)-Pd(1)	109.85(7)
S(1)-Pd(3)-Pd(1)	51.52(6)
P(3)-Pd(3)-Pd(1)	152.87(7)
S(2)-Pd(3)-Pd(2)	50.29(6)
S(1)-Pd(3)-Pd(2)	111.03(7)
P(3)-Pd(3)-Pd(2)	147.48(7)
Pd(1)-Pd(3)-Pd(2)	59.65(2)
C(1)-S(1)-Pd(3)	109.0(3)
C(1)-S(1)-Pd(1)	107.3(3)
Pd(3)-S(1)-Pd(1)	77.37(8)
C(13)-S(2)-Pd(3)	106.3(3)
C(13)-S(2)-Pd(2)	103.7(3)
Pd(3)-S(2)-Pd(2)	79.48(8)
C(7)-S(3)-Pd(1)	107.4(3)
C(7)-S(3)-Pd(2)	103.8(3)
Pd(1)-S(3)-Pd(2)	77.36(8)
O(3)-S(4)-O(2)	113.2(5)
O(3)-S(4)-O(1)	114.1(5)

O(2)-S(4)-O(1)	112.4(5)
O(3)-S(4)-C(73)	105.4(5)
O(2)-S(4)-C(73)	105.2(5)
O(1)-S(4)-C(73)	105.5(5)
C(25)-P(1)-C(19)	108.6(5)
C(25)-P(1)-C(31)	105.2(5)
C(19)-P(1)-C(31)	101.7(5)
C(25)-P(1)-Pd(1)	110.2(3)
C(19)-P(1)-Pd(1)	116.2(3)
C(31)-P(1)-Pd(1)	114.0(3)
C(49)-P(2)-C(37)	102.9(5)
C(49)-P(2)-C(43)	105.2(5)
C(37)-P(2)-C(43)	105.4(5)
C(49)-P(2)-Pd(2)	116.9(4)
C(37)-P(2)-Pd(2)	115.5(4)
C(43)-P(2)-Pd(2)	109.9(3)
C(61)-P(3)-C(55)	105.4(5)
C(61)-P(3)-C(67)	102.8(5)
C(55)-P(3)-C(67)	106.3(5)
C(61)-P(3)-Pd(3)	115.9(4)
C(55)-P(3)-Pd(3)	110.4(4)
C(67)-P(3)-Pd(3)	115.0(4)
C(82)-N(1)-C(86)	118.6(18)
C(82)-N(1)-C(85)	119.1(19)
C(86)-N(1)-C(85)	120.2(16)
N(3)-N(2)-C(76)	106.9(12)
N(2)-N(3)-C(79)	113.5(14)
C(3)-C(4)-Cl(2)	119.1(9)
C(5)-C(4)-Cl(2)	118.2(9)
C(8)-C(7)-S(3)	124.1(8)

C(12)-C(7)-S(3)	117.6(8)
C(11)-C(10)-Cl(1)	119.0(9)
C(9)-C(10)-Cl(1)	118.5(9)
C(14)-C(13)-S(2)	123.1(7)
C(18)-C(13)-S(2)	118.3(8)
C(15)-C(14)-C(13)	121.3(9)
C(15)-C(16)-Cl(3)	121.1(9)
C(17)-C(16)-Cl(3)	118.2(8)
C(24)-C(19)-P(1)	122.0(8)
C(20)-C(19)-P(1)	118.7(8)
C(23)-C(22)-F(1)	117.2(11)
C(21)-C(22)-F(1)	118.6(12)
C(26)-C(25)-P(1)	119.5(8)
C(30)-C(25)-P(1)	124.2(8)
C(29)-C(28)-F(2)	120.1(12)
F(2)-C(28)-C(27)	116.8(12)
C(32)-C(31)-P(1)	120.0(9)
C(36)-C(31)-P(1)	122.3(9)
C(33)-C(34)-F(3)	118.6(13)
C(35)-C(34)-F(3)	117.4(13)
C(38)-C(37)-P(2)	126.0(11)
C(42)-C(37)-P(2)	119.1(11)
C(39)-C(40)-F(4)	122.4(17)
C(41)-C(40)-F(4)	113.4(16)
C(44)-C(43)-P(2)	118.3(8)
C(48)-C(43)-P(2)	123.5(9)
C(47)-C(46)-F(5)	117.6(11)
C(45)-C(46)-F(5)	116.9(12)
C(50)-C(49)-C(54)	117.3(10)
C(50)-C(49)-P(2)	120.7(9)

C(54)-C(49)-P(2)	121.9(9)
C(51)-C(52)-F(6)	120.5(14)
C(53)-C(52)-F(6)	116.3(14)
C(60)-C(55)-P(3)	119.2(8)
C(56)-C(55)-P(3)	121.4(9)
C(59)-C(58)-F(7)	119.9(14)
C(62)-C(61)-P(3)	121.1(9)
C(66)-C(61)-P(3)	120.6(9)
C(65)-C(64)-F(8)	118.2(14)
C(68)-C(67)-P(3)	124.8(10)
C(72)-C(67)-P(3)	116.0(9)
C(69)-C(70)-F(9)	116.0(15)
C(71)-C(70)-F(9)	119.6(16)
C(74)-C(73)-S(4)	121.6(9)
C(78)-C(73)-S(4)	119.2(8)
C(77)-C(76)-N(2)	126.8(12)
C(75)-C(76)-N(2)	112.8(12)
C(84)-C(79)-N(3)	123.1(17)
C(80)-C(79)-N(3)	114.5(16)
C(81)-C(82)-N(1)	118(2)
C(83)-C(82)-N(1)	122.9(19)

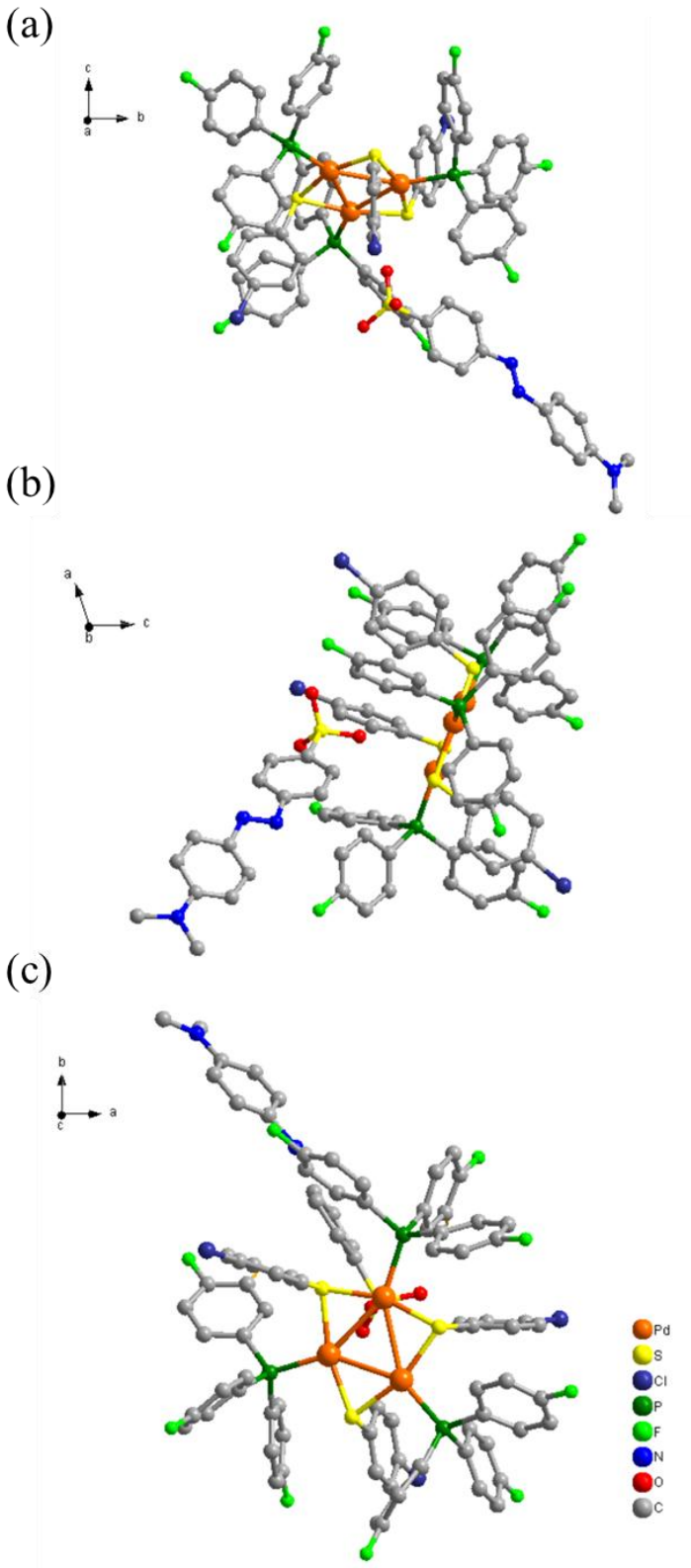

Fig. S6. The crystal structure of complex **7** displayed from a-axis perspective (a), b-axis perspective (b), and c-perspective (c), respectively.

9. FTIR for triangular palladium clusters 3-7

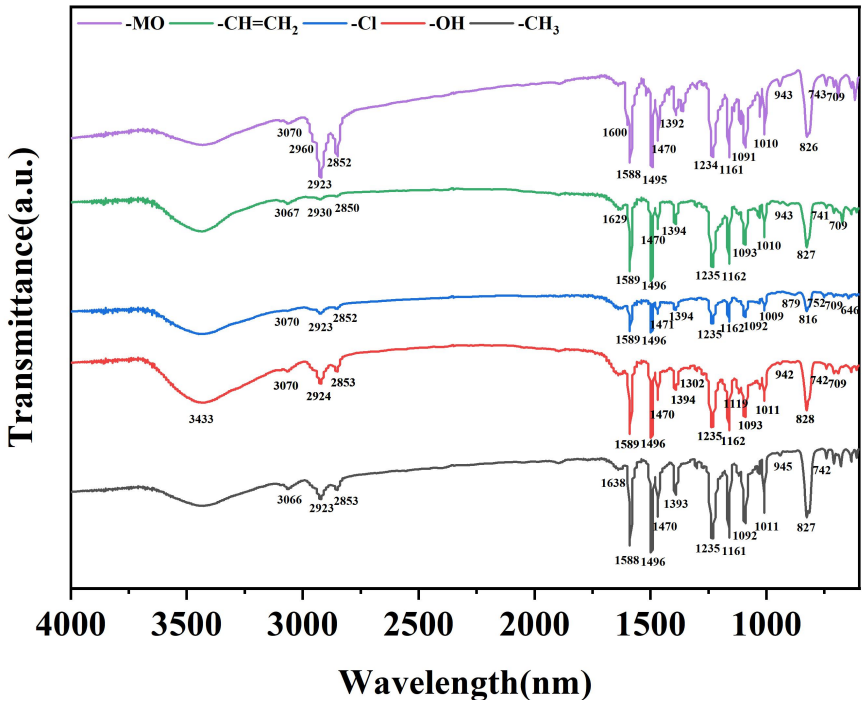

Fig. S7. IR (cm^{-1}) for **3** ($-CH_3$): v 3066, 2923, 2853, 1638, 1588, 1496, 1470, 1393, 1235, 1161, 1092, 1011, 945, 827, 742. IR (cm^{-1}) for **4** (-OH): v 3433, 3070, 2924, 2853, 1589, 1496, 1470, 1394, 1302, 1235, 1162, 1119, 1093, 1011, 942, 828, 742, 709. IR (cm^{-1}) for **5** (-Cl): v 3070, 2923, 2852, 1589, 1496, 1471, 1394, 1235, 1162, 1092, 1009, 879, 816, 752, 709. IR (cm^{-1}) for **6** ($-CH=CH_2$): v 3067, 2930, 2850,1629, 1589, 1496, 1470, 1394, 1235, 1162, 1093, 1010, 943, 827, 741, 709. IR (cm^{-1}) for **7** (-MO): v 3070, 2960, 2923, 2852, 1600, 1588, 1495, 1470, 1392, 1234, 1161, 1091, 1010, 943, 826, 743, 709.

10. UV-visible spectra for complexes 3-7 in MeOH

For comparison, we further measured the absorption for complexes (**3**-**7**) in MeOH (Fig. S8), their absorption intensity presented obvious solvent independence. Interestingly, complex **7** also presented red shift compared with complex **3** when MeOH was used as the solvent.

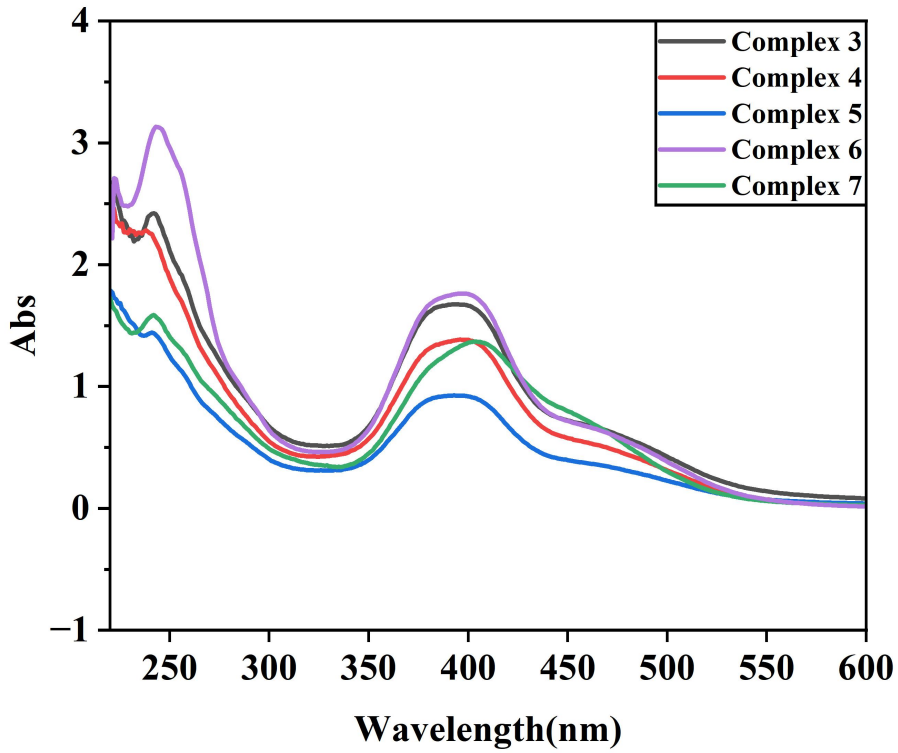

Fig. S8. The UV-visible spectra for complexes (**3**-**7**) in MeOH. For complex **3**: c = 1.0 × 10^{-4} mol/L, λ_{max1} = 242 nm (ε_{max1} = 2.4 × 10^4 $M^{-1}\cdot cm^{-1}$), λ_{max2} = 393 nm (ε_{max2} = 1.7 × 10^4 $M^{-1}\cdot cm^{-1}$). For complex **4**: c = 1.0 × 10^{-4} mol/L, λ_{max1} = 238 nm (ε_{max1} = 2.3 × 10^4 $M^{-1}\cdot cm^{-1}$), λ_{max2} = 399 nm (ε_{max2} = 1.4 × 10^4 $M^{-1}\cdot cm^{-1}$). For complex **5**: c = 1.0 × 10^{-4} mol/L, λ_{max1} = 241 nm (ε_{max1} = 1.4 × 10^4 $M^{-1}\cdot cm^{-1}$), λ_{max2} = 393 nm (ε_{max2} = 0.9 × 10^4 $M^{-1}\cdot cm^{-1}$). For complex **6**: c = 1.0 × 10^{-4} mol/L, λ_{max1} = 243 nm (ε_{max1} = 3.1 × 10^4 $M^{-1}\cdot cm^{-1}$), λ_{max2} = 397 nm (ε_{max2} = 1.8 × 10^4 $M^{-1}\cdot cm^{-1}$). For complex **7**: c = 1.0 × 10^{-4} mol/L, λ_{max1} = 242 nm (ε_{max1} = 1.6 × 10^4 $M^{-1}\cdot cm^{-1}$), λ_{max2} = 404 nm (ε_{max2} = 1.4 × 10^4 $M^{-1}\cdot cm^{-1}$).

11. Absorption and emission for the silver arylsulfonates 2a-e

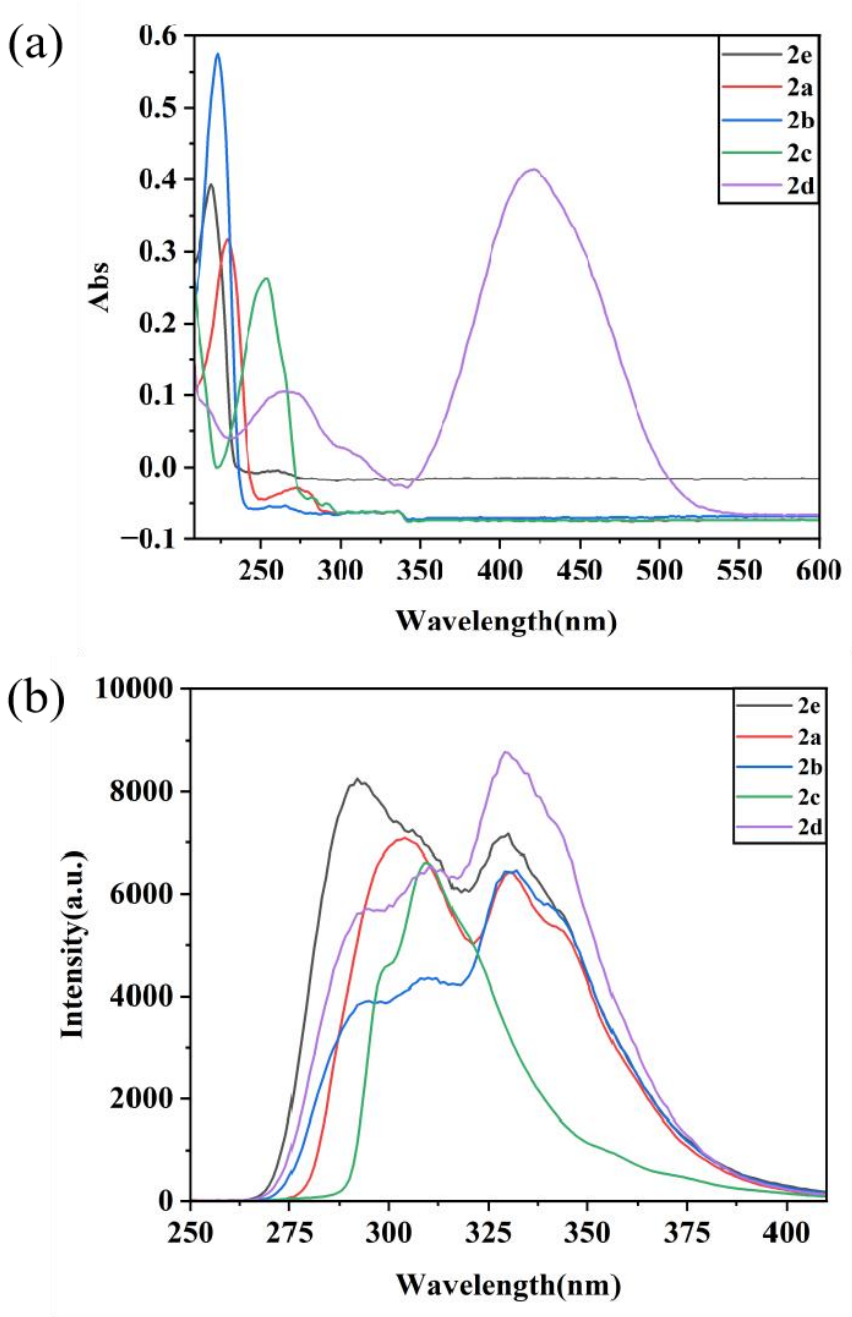

Fig. S9. (a) UV-visible spectra for the silver arylsulfonates **2a-e**. **2a**: c = 1.0 × 10^{-4} mol/L in CH_3OH, λ_{max} = 229 nm, ε_{max} = 0.32 × 10^4 $M^{-1}\cdot cm^{-1}$. **2b**: c = 1.0 × 10^{-4} mol/L in CH_3OH, λ_{max} = 223 nm, ε_{max} = 0.58 × 10^4 $M^{-1}\cdot cm^{-1}$. **2c**: c = 1.0 × 10^{-4} mol/L in CH_3OH, λ_{max} = 254 nm, ε_{max} = 0.26 × 10^4 $M^{-1}\cdot cm^{-1}$. **2d**: c = 1.0 × 10^{-4} mol/L in CH_3OH, λ_{max1} = 265 nm, λ_{max2} = 421 nm, ε_{max1} = 0.1 × 10^4 $M^{-1}\cdot cm^{-1}$, ε_{max2} = 0.42 × 10^4 $M^{-1}\cdot cm^{-1}$. **2e**: c = 1.0 × 10^{-4} mol/L in CH_3OH, λ_{max1} = 219 nm, ε_{max} = 0.39 × 10^4 $M^{-1}\cdot cm^{-1}$.(b) emission for the silver arylsulfonates **2a-e** in MeOH.

12. Photoluminescence Quantum Yields (PLQY) for complexes 3-7

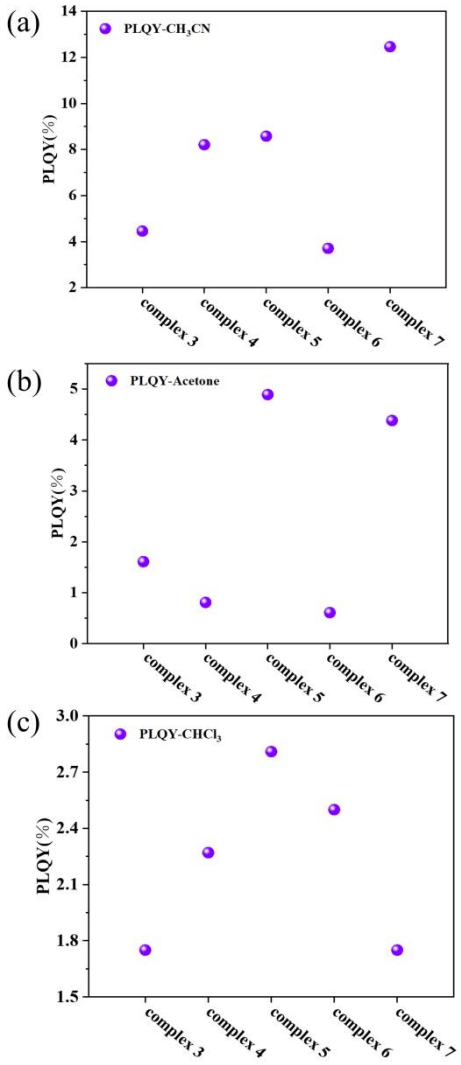

Fig. S10. (a) Photoluminescence Quantum Yields (PLQY) for complexes **3-7** (4.46%, 8.21%, 8.58%, 3.71%, 12.46%, respectively) in CH_3CN at room temperature (1×10^{-4} M). (b) PLQY for complexes **3-7** (1.61%, 0.81%, 4.89%, 0.61%, 4.38%, respectively) in CH_3COCH_3 at room temperature (1×10^{-4} M). (c) PLQY for complexes **3-7** (1.75%, 2.27%, 2.87%, 2.50%, 1.75%, respectively) in $CHCl_3$ at room temperature (1×10^{-4} M).

13. References

1) *SAINT Software Users Guide ,version 7.0*, Bruker Analytical X-Ray Systems, Madison, WI, 1999.
2) G. M. Sheldrick, *SADABS, version 2.03*, Bruker Analytical X-Ray Systems, Madision, WI, 2000.
3) G. M. Sheldrick, Crystal Structure Refinement with SHELXL. Acta Crystallogr., Sect. C: Struct. Chem. 2015, **71**, 3.
4) G. M. Sheldrick, *SHELXT, version 6.14*, Bruker AXS, Inc.,Madison, WI, 2000-2003.